AWARD NUMBER: W81XWH-17-1-0638

TITLE: Novel Therapeutic Target Identification through analysis of Convergent AD and TBI Pathogenic Mechanisms

PRINCIPAL INVESTIGATOR: Drs. Fiona Crawford/Joseph Ojo

CONTRACTING ORGANIZATION: The Roskamp Institute, Inc.
Sarasota, FL 34243-3922

REPORT DATE: October 2019

TYPE OF REPORT: Annual

PREPARED FOR: U.S. Army Medical Research and Materiel Command
Fort Detrick, Maryland 21702-5012

REPORT DOCUMENTATION PAGE

Form Approved
OMB No. 0704-0188

1. REPORT DATE: Oct 2019	**2. REPORT TYPE: Annual**	**3. DATES COVERED: 9/15/2018-9/14/2019**

4. TITLE AND SUBTITLE: Novel Therapeutic Target Identification through analysis of Convergent AD and TBI Pathogenic Mechanisms.

5a. CONTRACT NUMBER:

5b. GRANT NUMBER
W81XWH-17-1-0638

5c. PROGRAM ELEMENT NUMBER

6. AUTHOR(S)
Fiona Crawford, PhD – Main PI; Joseph Ojo, PhD – Co-PI; Catalina Gil – Grant Coordinator;

E-Mail: fcrawford@roskampinstitute.org; jojo@roskampinstitute.org; cgil@roskampinstitute.org;

5d. PROJECT NUMBER

5e. TASK NUMBER

5f. WORK UNIT NUMBER

7. PERFORMING ORGANIZATION NAME(S) AND ADDRESS(ES)
The Roskamp Institute, Inc., 2040 Whitfield Avenue Sarasota, FL 34243-3922

8. PERFORMING ORGANIZATION REPORT NUMBER

9. SPONSORING / MONITORING AGENCY NAME(S) AND ADDRESS(ES)

U.S. Army Medical Research and Materiel Command
Fort Detrick, Maryland 21702-5012

10. SPONSOR/MONITOR'S ACRONYM(S)

11. SPONSOR/MONITOR'S REPORT NUMBER(S)

12. DISTRIBUTION / AVAILABILITY STATEMENT

Approved for Public Release; Distribution Unlimited

13. SUPPLEMENTARY NOTES

14. ABSTRACT: Traumatic Brain Injury (TBI), in particular mild TBI (mTBI) is a major cause of disability in military and in civilian populations, and for many years has been known to be an epigenetic risk factor for Alzheimer's Disease (AD) and other neurodegenerative conditions. However, the precise nature of how TBI leads to or precipitates AD pathogenesis is not understood. To address this problem, we have generated molecular profiles of AD and TBI pathogenesis in mouse models at a range of ages/timepoints post-injury respectively, in order to identify molecules and pathways that are common to both AD and TBI. Extensive datasets have been generated, and our comparison and integration of omic profiles clearly points to overlapping disruption of brain lipids and related protein signaling pathways in AD mice with age and TBI mice with time post injury. These include activation of lipid related leukotriene signaling, deficiencies in the eicosanoid signaling, dysfunctional PI3-kinase/Akt/mTOR/insulin and RXR/PPAR pathway. Lipids, particularly phospholipids are essential components of neuronal and glial cell membranes and axonal myelin, they modulate protein-protein interaction and cell signal transduction. Thus the TBI-induced pathobiology we have observed may precipitate development of AD and lower the threshold for onset of pathogenic mechanisms. We therefore now propose to validate these convergent AD and TBI mechanisms as novel targets to block the negative sequelae of TBI that lead to AD.

15. SUBJECT TERMS: AD, TBI, Pathology, Animal Models, Novel Therapeutic Targets

16. SECURITY CLASSIFICATION OF:			**17. LIMITATION OF ABSTRACT**	**18. NUMBER OF PAGES**	**19a. NAME OF RESPONSIBLE PERSON**
a. REPORT	**b. ABSTRACT**	**c. THIS PAGE**			USAMRMC
Unclassified	Unclassified	Unclassified	Unclassified	**48**	**19b. TELEPHONE NUMBER** *(include area code)*

Table of Contents

1. INTRODUCTION

In this new project we plan to identify and provide preliminary validation of novel targets (eicosanoid signaling, dysfunctional PI3-kinase/Akt/mTOR/insulin and RXR/PPAR pathway) for the TBI-AD interrelationship discovered through our molecular level profiling. The goal here is target validation and provision of these therapeutic targets for future studies in drug discovery and preclinical efficacy; i.e. IND enabling studies of new therapeutic approaches to the AD sequelae of TBI.

2. KEY WORDS: AD, TBI, Pathology, Animal Models, Novel Therapeutic Targets

3. KEY RESEARCH ACCOMPLISHMENTS

OVERALL PROJECT SUMMARY

Traumatic Brain Injury (TBI), in particular mild TBI (mTBI) is a major cause of disability in military and in civilian populations, and for many years has been known to be an epigenetic risk factor for Alzheimer's Disease (AD) and other neurodegenerative conditions. However, the precise nature of how TBI leads to or precipitates AD pathogenesis is not understood. To address this problem, we have generated molecular profiles of AD and TBI pathogenesis in mouse models at a range of ages/timepoints post-injury respectively, in order to identify molecules and pathways that are common to both AD and TBI. Extensive datasets have been generated, and our comparison and integration of omic profiles clearly points to overlapping disruption of brain lipids and related protein signaling pathways in AD mice with age and TBI mice with time post injury. These include activation of lipid related leukotriene signaling, deficiencies in the eicosanoid signaling, dysfunctional PI3-kinase/Akt/mTOR/insulin and RXR/PPAR pathway. Lipids, particularly phospholipids are essential components of neuronal and glial cell membranes and axonal myelin, they modulate protein-protein interaction and cell signal transduction. Thus the TBI-induced pathobiology we have observed may precipitate development of AD and lower the threshold for onset of pathogenic mechanisms. We therefore now propose to validate these convergent AD and TBI mechanisms as novel targets to block the negative sequelae of TBI that lead to AD.

Objective/Hypothesis: Molecular pathways that are triggered in response to both TBI sequelae and AD pathogenesis represent novel molecular targets to mitigate the AD-neurodegenerative sequelae of TBI.
From our interrogation of omic datasets of AD pathogenesis and TBI sequelae we have identified coincident lipid disturbances and related pathways which are potential targets for therapeutic intervention. Therefore we propose to first: **Aim 1:** Evaluate target engagement and efficacy in recovering normal molecular profiles in TBI mice using compounds that modulate the TBI and AD coincident molecular changes in a short-term treatment paradigm. **Aim 2:** In vivo validation of therapeutic targets in mice with TBI using chronic intervention with the top three performing compounds for three different targets from Aim 1 to evaluate the long term neurobehavioral, neuropathological and biochemical consequences.

The major goals of the project?

Major Task 1: Validation of potential targets for therapeutic intervention in the pathogenic TBI-AD interrelationship - eicosanoid signaling, PI3-kinase/Akt/PTEN/mTOR/insulin signaling and RXR/PPAR pathway.

Major Task 2: Chronic evaluation of the efficacy of three potential therapeutics against the pathogenic TBI-AD interrelationship

SUMMARY OF ACCOMPLISHMENTS

At the start of the year we began interrogation of target engagement and therapeutic efficacy (i.e. ability to ameliorate glial reactivity, axonal and white matter changes in our TBI model) of administered compounds Monteleukast (leukotriene receptor antagonist), Zileuton (5-lipo-oxygenase inhibitor), flavonoid 7,8-dihydroxyflavone (BDNF receptor-TrkB agonist), and Fingolimod (sphingosine-1-phosphate receptor modulator), Oleoylethanolamide (PPARα agonist), Pioglitazone (PPARγ agonist), intranasal insulin, Baxerotene (RXR agonist) and Liraglutide (IGF1/GLP-1). Our final target is PTEN/mTOR, we are using a transgenic mouse model to currently explore the potential of this target in our TBI model, as we considered our invasive approach to be unsuitable in vivo, data will be analyzed by December 2020. All data have been completed for the major aspects of our first aim, and we plan to initiate the second Aim focusing on three top performing compounds in a chronic treatment paradigm using our TBI model.

During this year, we also validated our main targets in human autopsy TBI and AD tissue to demonstrate human relevance.

We finished the development of a mass spectrometry protocol for measuring bioactive lipids in the brain tissue and isolated single cells of TBI vs sham mice to validate changes in downstream bioactive lipids related to the eicosanoid pathways. This assay will potentially be used to screening >25 bioactive lipids such as – lipoxins, arachidonic acid, leukotrienes, D and E –series resolvins, decosahexaenoic acid, eicosapentaenoic acid, 18-HEPE, prostaglandins, and primary eicosanoids e.g. thromboxanes etc. We also developed a single cell isolation method for extracting glial cells for interrogation of cell specific effects in our model. We plan to use this single cell analyses to interrogate proteomic and lipidomic effects of our compounds in microglia and astrocytes for our long-term treatment study.

We have also included as part of this project an additional in vitro screening platform for our compounds in astrocyte, microglia and neuronal cell lines. We have developed a timeline of pathological profiles of inflammation, tau, axonal injury etc... in these cell culture models, which we will use to screening the efficacy of some of our top performing compounds. Our goal is to utilize this platform as an additional validation step in the selection of our top performing compounds prior to initiating our long term treatment studies in Aim 2. We plan to complete these studies within the next three months. We will rank the list of different compounds and use our statistical method for selecting the best performing.

What have we accomplished under the Major goals?

As detailed above, we have accomplished almost all of the subtasks related to MAJOR TASK 1 (please see below for the list of subtasks relating to both MAJOR TASKS 1 and 2).
Efforts from SUBTASK 1 to 3/4 were completed in the previous Annual report.
In this reporting period we have accomplished almost all efforts from SUBTASK 4 to 7.
We are also currently breeding and ageing mice, and planning administration of injuries for the start of studies in Major Task 2, where we will administer the top 3 performing compounds in a long-term treatment regimen that will be initiated 3 months post-injury and last for 6 months until euthanasia. In this study we will conduct behavioral, neuropathological, and biochemical analyses to asses efficacy of our compounds.

SUBTASK DESCRIPTIONS FOR MAJOR TASK 1

Subtask 1: Obtained ACURO approval (completed in March 20th, 2018)
Subtask 2: Evaluation of bioactive lipids and downstream signaling in stored TBI and AD mouse model samples to identify proposed targets from Leukotriene and Sphingomyelin signaling
Subtask 3: Administration of r-mTBI or r-sham injury to 180-220 male C57BL6/J mice at 2-3 months of age
Subtask 4: Administration of therapeutic compounds to C57BL6/J mice for 2 weeks immediately prior to 2 month timepoint post-TBI/sham.
Subtask 4a-d: Administration of therapeutic compounds to target (eicosanoid signaling, PI3-kinase/Akt/PTEN/mTOR/insulin signaling and RXR/PPAR pathway)
Subtask 4e: Target exploration of downstream eicosanoid pathway and administration of therapeutic compounds to target leukotriene signaling
Subtask 4f: Target exploration of downstream sphingomyelin pathway and administration of therapeutic compounds to target sphingomyelin signaling
Subtask 5: Euthanasia of hTau mice at 3 months post-TBI/sham, followed by brain omic and antibody based analyses
Subtask 6: Validation of identified targets in human TBI brains with history of repetitive concussions
Subtask 7: Evaluation and selection of therapeutics for each target for use in Task 2

MAJOR TASK 1 DELIVERABLE: Acute study validation of coincident TBI and AD molecular targets and verification of up to 8 compounds as engaging those targets *in vivo.*
Selection of Top 3 performing compounds for study in MAJOR TASK 2.

SUBTASK DESCRIPTIONS FOR MAJOR TASK 2

Subtask 1: Administration of r-mTBI or r-sham injury to 180 male hTau mice at 2-3 months of age (60 mice per group)
Animals will receive closed head injuries over a 1 month period.
For each of 3 potential therapeutics there will be 6 groups– [r-mTBI treated low dose; r-mTBI treated high dose; r-mTBI vehicle; r-sham treated low dose; r-sham treated high dose; r-sham vehicle] each with 10 hTau mice
Subtask 2: Administration of therapeutic compounds to hTau mice for 6 months beginning at 3 months post TBI/sham.
Subtask 2a: Administration of Top performing therapeutic compound I
Subtask 2b: Administration of Top performing therapeutic compound II
Subtask 2c: Administration of Top performing therapeutic compound III

Subtask 3: Neurobehavioral testing of hTau mice in the two weeks prior to 9 months post injury timepoint
At the last two weeks prior to the 9 month post-injury time-point, animals will undergo neurobehavioral testing in the Barnes maze for 7 days, followed by rotarod test , open field and elevated plus maze tests.
Subtask 4: Euthanasia of hTau mice at 9 months post-TBI/sham, followed by further evaluation of outcomes
Subtask 4a: Brain neuropathological analyses
Subtask 4b: Omics and antibody based analyses
Subtask 5: Data analysis and interpretation to identify most potent therapeutic approach

MAJOR TASK 2 DELIVERABLE: Chronic study validation of top three candidate treatments that rescue TBI-dependent sequelae from convergence with AD pathogenic mechanisms.

BELOW IS A SUMMARY OF THE MAIN FINDINGS FROM OUR STUDIES THIS YEAR

Repetitive mTBI is associated with reactive microgliosis

To verify that our 20-hit injury paradigm was sufficient to induce reactive gliosis, we assessed the immunophenotype of microglia within the brains of sham vehicle treated and TBI vehicle treated mice (N=3 per group). Following the enzymatic digestion of mouse brain tissue to generate a single cell suspension cells were stained with anti-CD11b FITC, anti-CD45-PE and anti-CX3CR1-CY5.5. Cells were gated using forward and side scatter to select for single cells and then assessed on their expression of these markers (Fig 1A-B). Significance was assessed by *Students T test* and when positive fractions were normalized for total cell count, a significant increase in CD45 (P=0.035) (FIG.1C), and CX3CR1 (P=0.0108) (FIG.1D) was noted between sham and TBI groups.

After determining that the injury paradigm is suitable to induce reactive gliosis, a well described feature of mTBI, we sought to investigate if the pharmacological blockade of leukotrienes could ameliorate the pathology associated with r-mTBI.

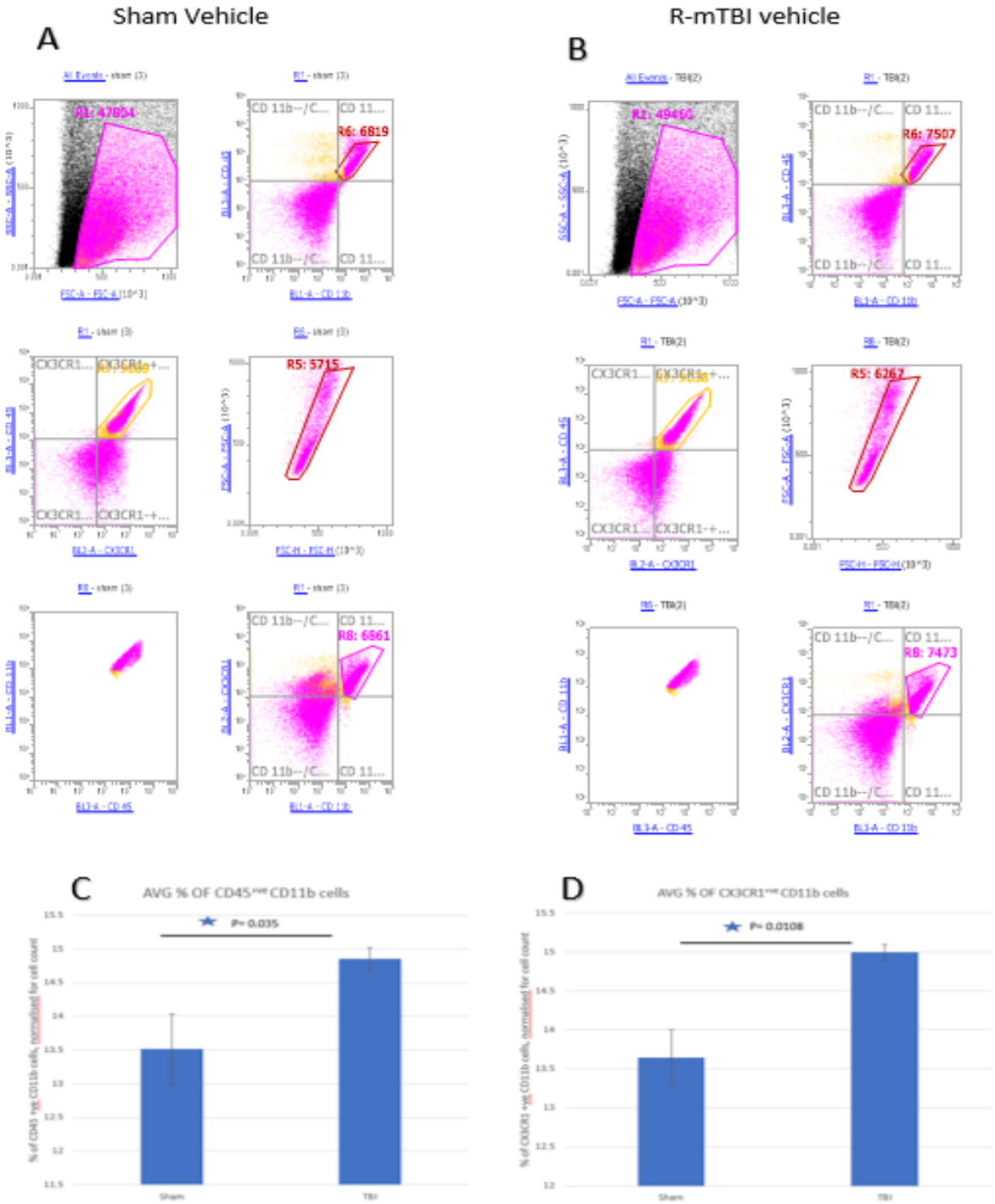

Figure.1. Activation dynamics of CD11b^{+ve} microglia and macrophages after 20-hit injury paradigm vs. sham C57BL/6 (Wild type) mouse whole brain. Representative image readout of sham (A) and injured (B) mice following flow cytometry analysis of Bivariate dot plots ofCD11b^{+ve} cells separated using a 30-70% percoll gradient to generate a mixed glial cell population. Quantification of CD11b^{+ve} against CD45^{+ve} expression (C), and CD11b^{+ve} against CX3CR1 expression (D). Data are expressed as ± standard error of the mean (n=3 per group). Data were assessed by students T test and significance between groups is indicated on the graph. (= P<0.05; **= P<0.01).*

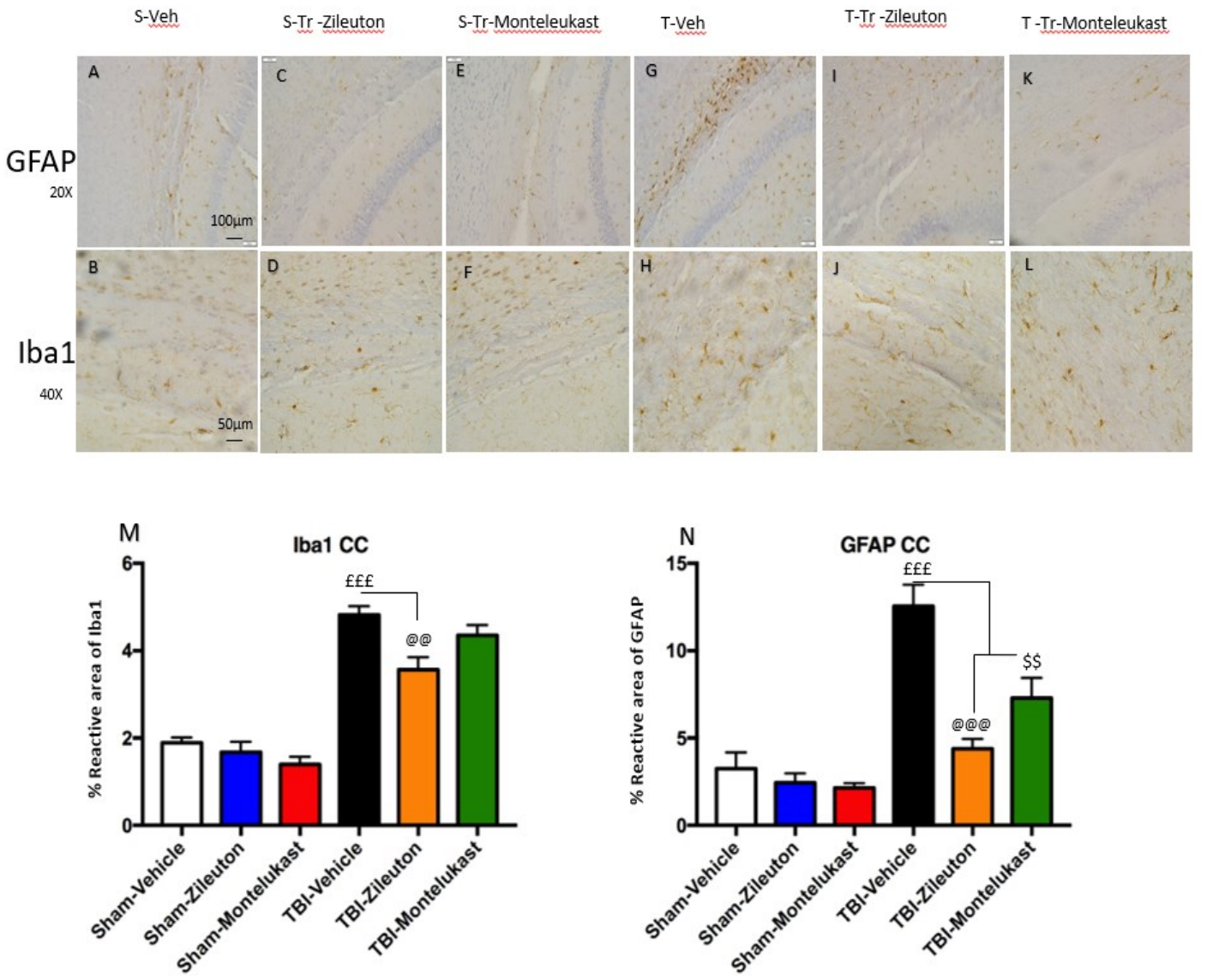

Figure.2. Neuropathological analysis of GFAP and IBA1 in the corpus callosum of C57BL/6 (Wild type) mice following 20-hit injury paradigm or sham procedure, and treatment with zileuton(32mg/kg/day) or Montelukast (10mg/kg/day). Sham Vehicle group GFAP (A), Iba1(B), Sham treated with zileuton (S-Tr-Zileuton) group GFAP (C), Iba1(D), Sham treated with Montelukast (S-Tr-Montelukast) group GFAP (E), Iba1(F), mTBI vehicle (T-Veh) group GFAP (G), Iba1(H), mTBI treated with zileuton (T-Tr-Zileuton) group GFAP (I), Iba1 (J), and mTBI treated with Montelukast (T-Tr-Montelukast) group GFAP (K), Iba1 (L). Scale bars at 20x magnification represent 100um and 50um at 40x magnification. Quantification of % reactive area of Iba1^{+ve} cells in 6 non-overlapping images taken along the body of the Corpus callosum (M), data were analysed by One-way ANOVA and p= 0.001. Quantification of % reactive area of GFAP^{+ve} cells in 6 non-overlapping images taken along the body of the Corpus callosum (N), data were analysed by One-way ANOVA and p =0.0001. Data are expressed as ± standard error of the mean (n=6 per group). Significance between Sham vehicle vs. TBI vehicle group represented by (£), significance assessed to be p=0.001 represented by £££. TBI vehicle vs. TBI treated with Zileuton group is represented by (@), significance assessed to be p=0.001 represented as @@@. TBI vehicle vs. TBI treated with Montelukast group is represented by $, Significance assessed to be p=0.01, represented as $$.

Pharmacological blockade of leukotrienes ameliorates reactive gliosis in the hippocampus and corpus callosum induced by repetitive mTBI induces.

From previous work investigating the pathological effects of our mTBI model, we have identified that the white matter is particularly susceptible to injury, therefore we primarily focus on the Corpus callosum.

Consistent with our previous models of mTBI, mice subjected to injury display evidence of a robust astrogliosis within the corpus callosum compared to shams (P=0.0001) (Fig.2.N). This prominent astrogliosis was subsequently rescued via treatment with Zileuton (P=0.001) and Montelukast (P=0.001). A similar response was seen when examining Iba1+ve cells, r-mTBI induced microgliosis within the Corpus callosum compared against shams (P= 0.001) and again this was subsequently rescued by Zileuton administration (P=0.01) (Fig.2.M). See Fig 2A-L for representative images of IBA1 and GFAP.

Similar to data from the Corpus callosum, we identified a robust astrogliosis throughout the hippocampus (Fig. 3. A, D). We proceeded to probe the Astrocyte response to Repetitive mTBI via immunoblotting, where we identified that TBI induced a robust astrogliosis (P=0.001) compared to shams (Fig.3. G). Administration of Zileuton or montelukast to injured animals resulted in a significant decrease in hippocampal astrogliosis (P=0.0018) and (P=0.006) respectively (Fig. 3. H). See Fig 3A-F for representative images of GFAP.

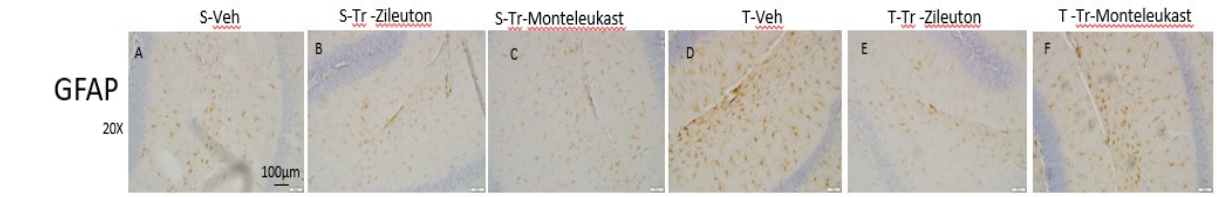

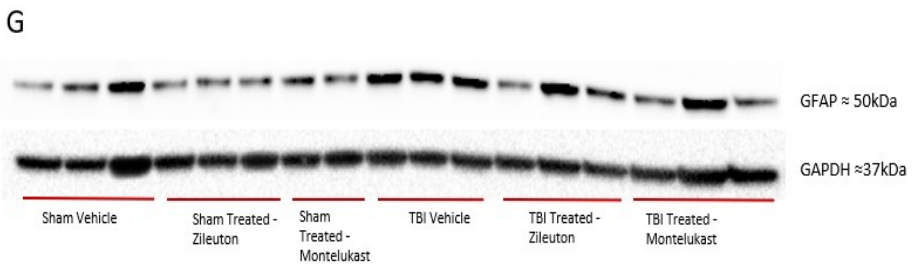

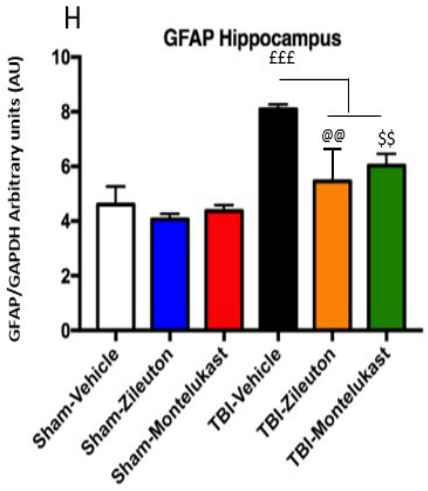

Figure.3. Neuropathological analysis of GFAP in the hippocampus of C57BL/6 (Wild type) mice following 20-hit injury paradigm or sham procedure, and treatment with zileuton(32mg/kg/day) or Montelukast (10mg/kg/day). Sham Vehicle group GFAP (A), Sham treated with zileuton (S-Tr-Zileuton) group GFAP (B), Sham treated with Montelukast (S-Tr-Montelukast) group GFAP (C), mTBI vehicle (T-Veh) group GFAP (D), mTBI treated with zileuton (T-Tr-Zileuton) group GFAP (E), and mTBI treated with Montelukast (T-Tr-Montelukast) group GFAP (F), . Scale bars at 20x magnification represent 100um and 50um at 40x magnification. (G) Representative western blot of hippocampal tissue when stained for anti GFAP and normalized against anti-GAPDH. (H) Quantitative representation of (Fig.G). Data are expressed as ± standard error of the mean (n=6 per group). Significance between Sham vehicle vs. TBI vehicle group represented by (£), significance assessed to be p=0.001 represented by £££. TBI vehicle vs. TBI treated with Zileuton group is represented by (@), significance assessed to be p=0.01 represented as @@. TBI vehicle vs. TBI treated with Montelukast group is represented by $, Significance assessed to be p=0.01, represented as $$.

Zileuton reduces 5-LOX protein expression and inhibits leukotriene synthesis

To confirm that the effects on pathology identified by immunohistochemistry were as a result of 5-Lipoxygenase inhibition, we performed quantitative protein expression analysis via western blotting on the cortex of each group (n=6 per group) to determine the protein expression of 5-LOX in sham and injured mice both vehicle treated and treated with the zileuton or montelukast. (FIG.4. A and B) TBI vehicle mice demonstrated a significantly increased 5-LOX expression compared to sham vehicle mice (P=0.003). Treatment with Zileuton following TBI significantly reduces 5-LOX protein expression compared to TBI vehicle (P=0.001) to those of sham vehicle groups, which can be seen by the lack of significance between these two groups. Treatment with Montelukast had no effect on 5-LOX expression in either sham or TBI groups relative to their vehicle counterparts.

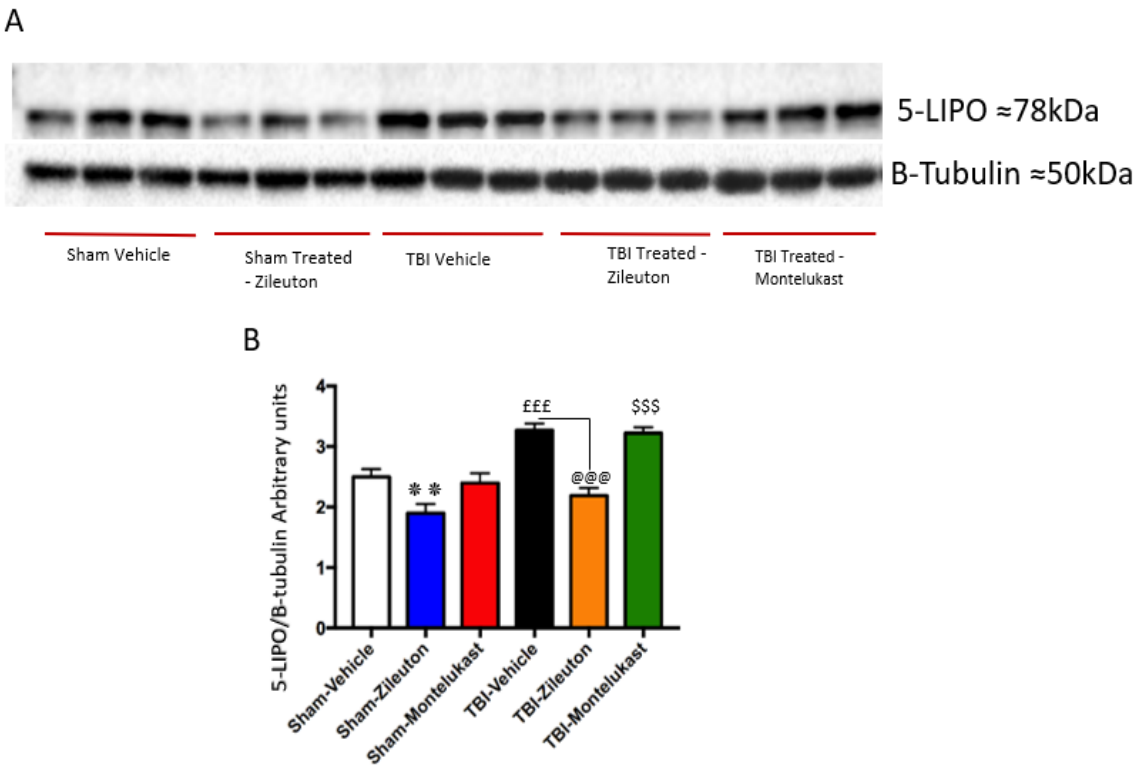

*Figure.4. 5-LOX protein expression in C57BL/6 (Wild type) mice following 20-hit injury paradigm or sham procedure, and treatment with zileuton(32mg/kg/day) or Montelukast (10mg/kg/day) analysis of mouse brains following Injury and treatment. (A) Representative western blotting of 20 hit mTBI mice cortex samples. (B) of Figure A, data were analysed by One-way ANOVA and p =0.0001. Data are expressed as ± standard error of the mean (n=6 per group. Significance between Sham vehicle vs. TBI vehicle group represented by (£), significance assessed to be p=0.001 represented by £££. TBI vehicle vs. TBI treated with Zileuton group is represented by (@), significance assessed to be p=0.001 represented as @@@. TBI vehicle vs. TBI treated with Montelukast group is represented by $, Significance assessed to be p=0.001, represented as $$$. Significance between Sham vehicle vs. Sham treated with Zileuton is represented at *, significance assessed to be p=0.01 represented as (**).*

Repetitive mTBI induces NFkB activation which is inhbitited by zileuton administration

Due to the key role of NFkB in CNS inflammation we sought to investigate the effect of our 20-hit paradigm and subsequent treatment on NFkB expression and activation (P-NFkB/ T-NFkB), assessed via western blotting of the cortex of each group (n=6 per group) - Fig.5. A. While no changes were seen in Total NFkB levels (Fig.5.B). Mice within the TBI vehicle group demonstrated a significant increase in P-NFkB/ T-NFkB ratio compared to sham vehicle mice (P=0.001) (FIG.5.C). Treatment with Zileuton following mTBI significantly reduced P-NFkB/ T-NFkB ratio (P=0.007) back to sham levels which can be seen by the lack of difference between Sham vehicle and TBI treated-Zileuton groups (P=0.147) (FIG.5.C). Similarly the administration of Montelukast to mTBI-injured animal also significantly reduced NFkB activation (P=0.0176) (FIG.5.C).

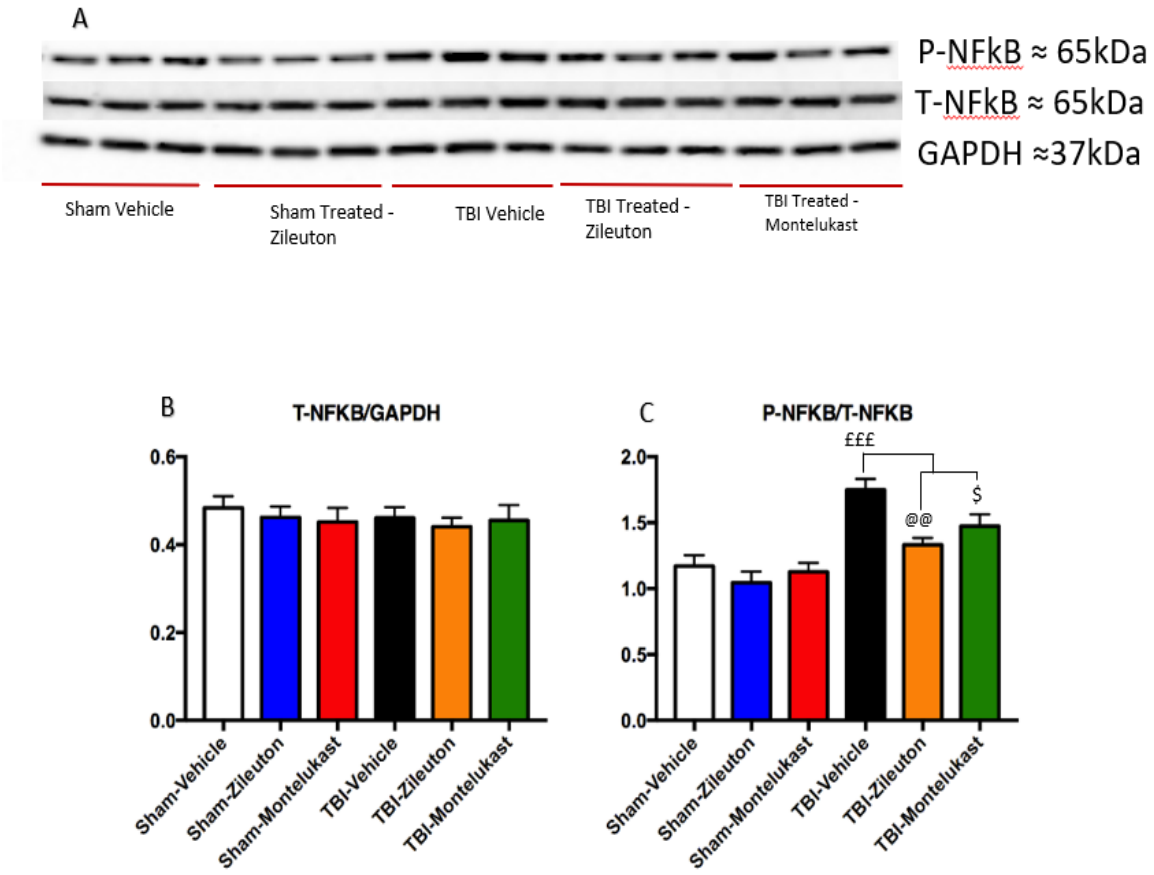

Figure.5. Total NFkB (T-NFkB) and Phospho NFkB (P-NFkB) expression in C57BL/6 (Wild type) mice following 20-hit injury paradigm or sham procedure, and treatment with zileuton(32mg/kg/day) or Montelukast (10mg/kg/day) analysis of mouse brains following Injury and treatment. (A) Representative western blotting of 20 hit mTBI mice cortex samples. (B) of Figure A, data were analysed by One-way ANOVA and p =0.0001. Data are expressed as ± standard error of the mean (n=6 per group). (Figure.C.) Significance between Sham vehicle vs. TBI vehicle group represented by (£), significance assessed to be p=0.001 represented by £££. TBI vehicle vs. TBI treated with Zileuton group is represented by (@), significance assessed to be p=0.007 represented as @@. Significance between Sham vehicle vs. TBI treated with Montelukast is represented by ($) significance assessed to be p=0.0176, represented as ($).

Repetitive mTBI increase total tau (DA9)

Several post mortem analyses of the brains of those who have suffered r-mTBI have reported an increase in Tau levels, and tau Phosphorylation (McKee et al., 2015). We therefore, sought to investigate the potential of our model to induce Tau pathology. Tau protein levels were assessed by western blotting of cortex tissue from each group (n=6 per group) – Fig.6.A. In this mode of r-mTBI we found a significant increase in total tau (DA9) in injured groups compared to shams (0.0056) - Fig.6.B. Treatment with zileuton or montelukast had no significant effect on DA9 levels in either group (Fig.6.B). Furthermore, while we did not see a significant increase in RZ3 for TBI vehicle mice (Fig.6.C) (P=0.086), mice treated with Zileuton and Montelukast did however demonstrate a reduced expression of phosphorylated Tau (RZ3) (p=0.011) and (P=0.002) respectively, when compared against TBI vehicle mice.

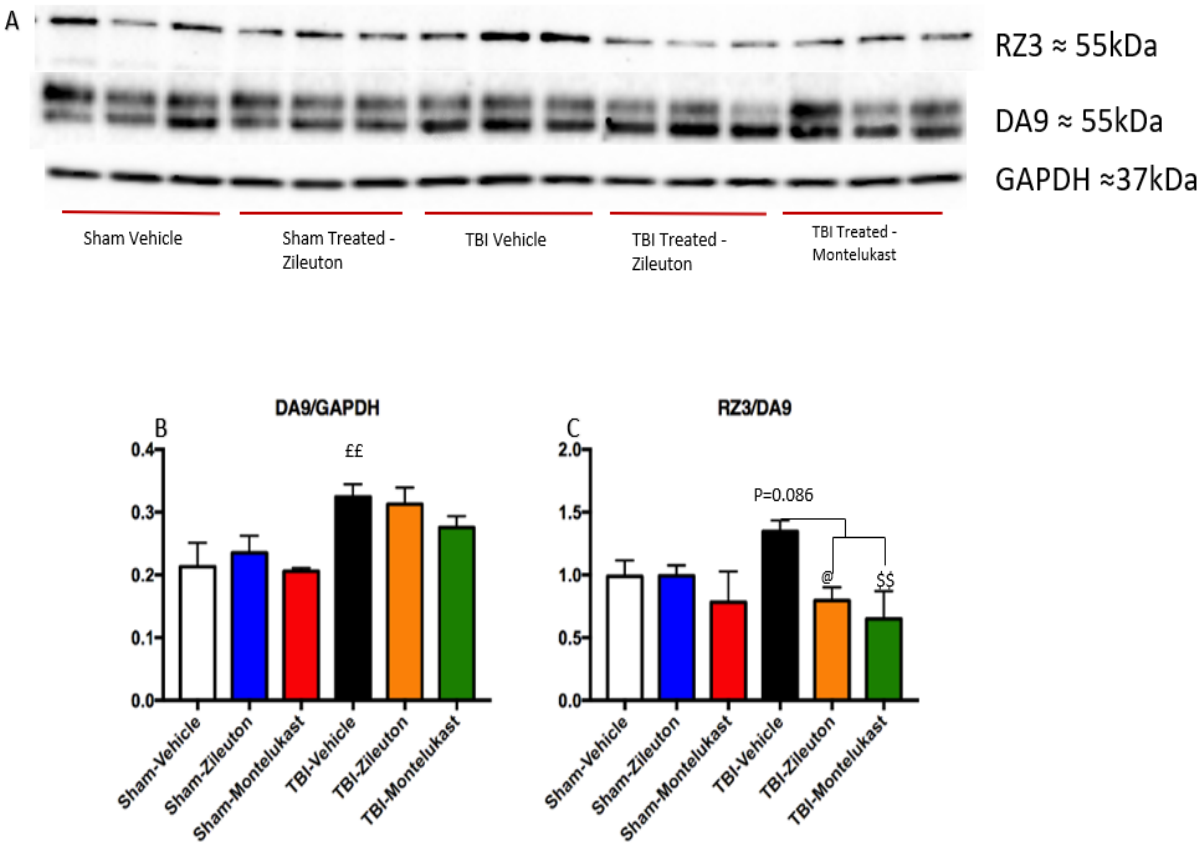

Figure.6. Total TAU (DA9) and Phospho Tau (RZ3) expression in C57BL/6 (Wild type) mice following 20-hit injury paradigm or sham procedure, and treatment with zileuton(32mg/kg/day) or Montelukast (10mg/kg/day) analysis of mouse brains following Injury and treatment. (A) Representative western blotting of 20 hit mTBI mice cortex samples. (B) of Figure A, data were analysed by One-way ANOVA and p =0.0001. Data are expressed as ± standard error of the mean (n=6 per group. Significance between Sham vehicle vs. TBI vehicle group represented by (£), significance assessed to be p=0.0056 represented by ££ (Fig.8.B) and p=0.086 represented (Fig.8.C). TBI vehicle vs. TBI treated with Zileuton group is represented by (@), significance assessed to be p=0.011 represented as @. @@. Significance between Sham vehicle vs. TBI treated with Montelukast is represented by ($) significance assessed to be p=0.002, represented as ($$).

Repetitive mTBI upregulates CDK5 which is reduced by zileuton administration

After we determined that the pharmacological blockade of leukotrienes suggested a reduction in Tau phosphorylation we began to seek a potential mechanism for this reduced Tau phosphorylation. While we did not find any substantial changes in P-GSK3b (Data not shown), we did however identify a TBI effect with regards to Cyclin-dependent Kinase (CDK5) a protein kinase well described to phosphorylate Tau in conditions such as CTE (Lucke-Wold et al., 2014). TBI vehicle mice demonstrated a significance increase in CDK5 expression (P=0.001) when compared to sham vehicle mice (Fig.7.A, B). This was subsequently rescued by administration of zileuton (P=0.001) and montelukast (p=0.01).

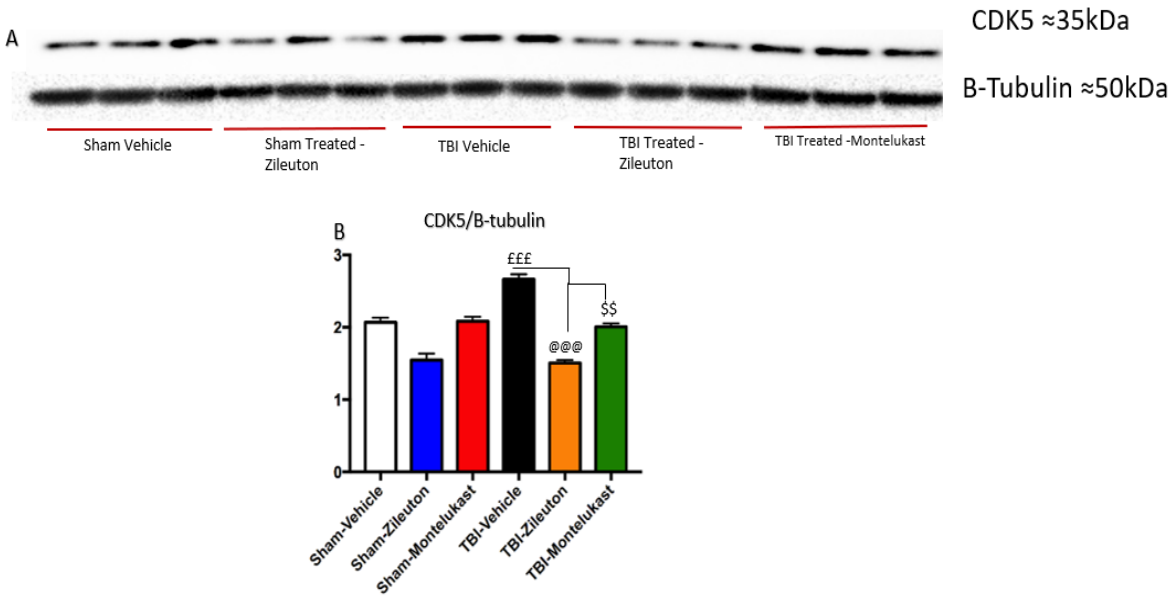

Figure.7. CDK5 expression in C57BL/6 (Wild type) mice following 20-hit injury paradigm or sham procedure, and treatment with zileuton (32mg/kg/day) or Montelukast (10mg/kg/day) analysis of mouse brains following Injury and treatment. (A) Representative western blotting of 20 hit mTBI mice cortex samples. (B) of Figure A, data were analysed by One-way ANOVA and p =0.0001. Data are expressed as ± standard error of the mean (n=6 per group. Significance between Sham vehicle vs. TBI vehicle group represented by (£), significance assessed to be p=0.001 represented by £££ (Fig.9.B) and p=0.086 represented (Fig.8.C). TBI vehicle vs. TBI treated with Zileuton group is represented by (@), significance assessed to be p=0.001 represented as @. @@. Significance between Sham vehicle vs. TBI treated with Montelukast is represented by ($) significance assessed to be p=0.01, represented as ($$).

Pharmacological blockade of TrkB receptor after repetitive mTBI

>Minimal effects of 7,8-Dihydroxyflavone on BDNF/TrkB signaling. [Figure 8A-F]
>7,8-Dihydroxyflavone does not mitigate iNOS increase post-injury. [Figure 8G]
>7,8-Dihydroxyflavone attenuates TBI-mediated astrogliosis in the corpus callosum. [Figure 9]

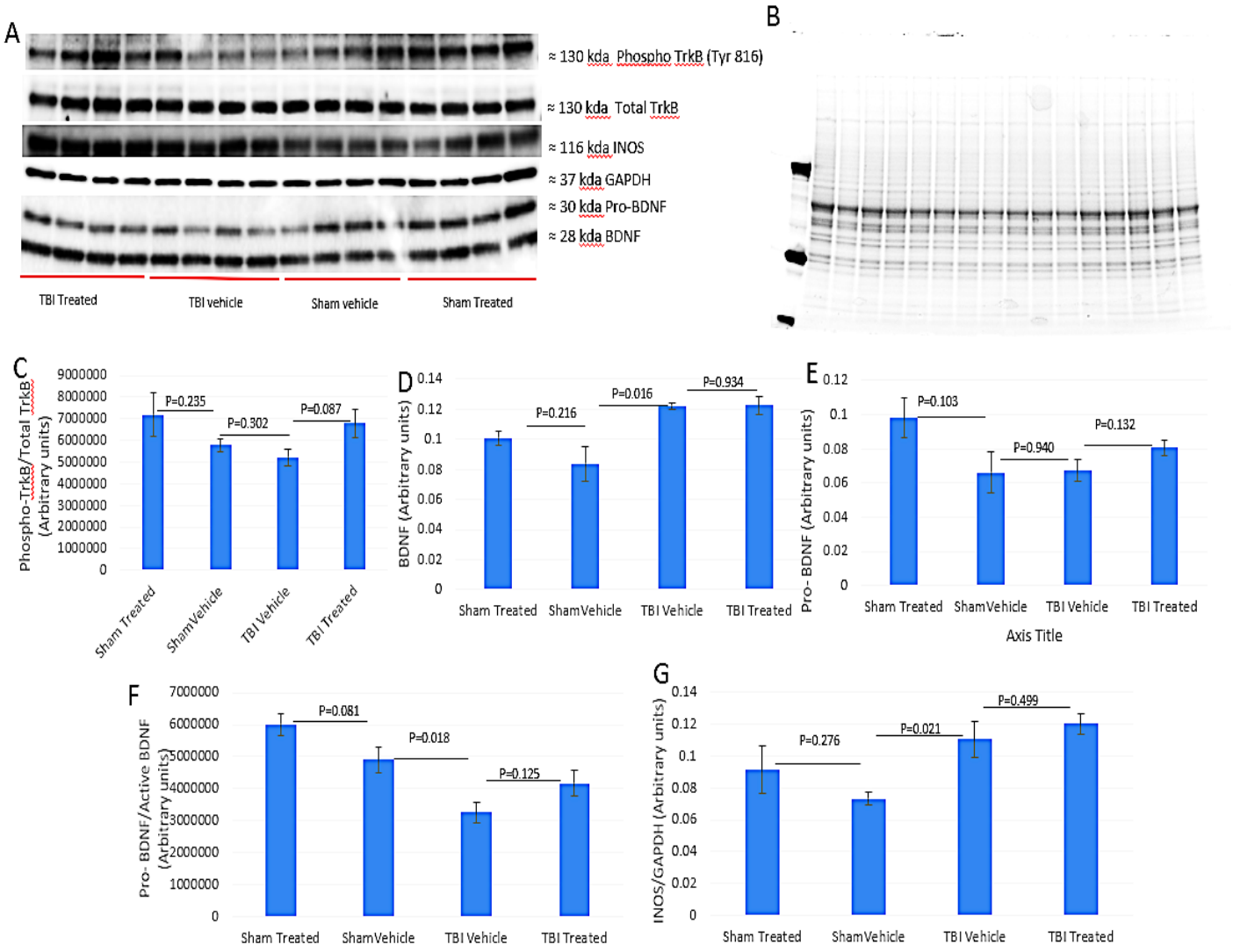

Figure.8. A) Immunoblot image showing representative results from cohort 3, Showing protein level expression of Phospho-TrkB, Total TrkB, Inducible Nitric oxide synthase (INOS), Pro and active BDNF and GAPDH (Housekeeping gene). B) Stain free image of gel electrophoresis used as a further normalization control. C) Graph showing Protein expression of Phospho-TrkB / Total TrkB. D) Graph showing protein expression of Active BDNF. E) Graph showing protein expression of Pro-BDNF. F) Graph showing ratio of Pro-BDNF/ Active BDNF to demonstrate processing into active BDNF. G) graph showing protein expression of INOS. n=4 per group, error bars are shown as standard error of the mean (SEM) and data was statistically analyzed using a Students T-Test.

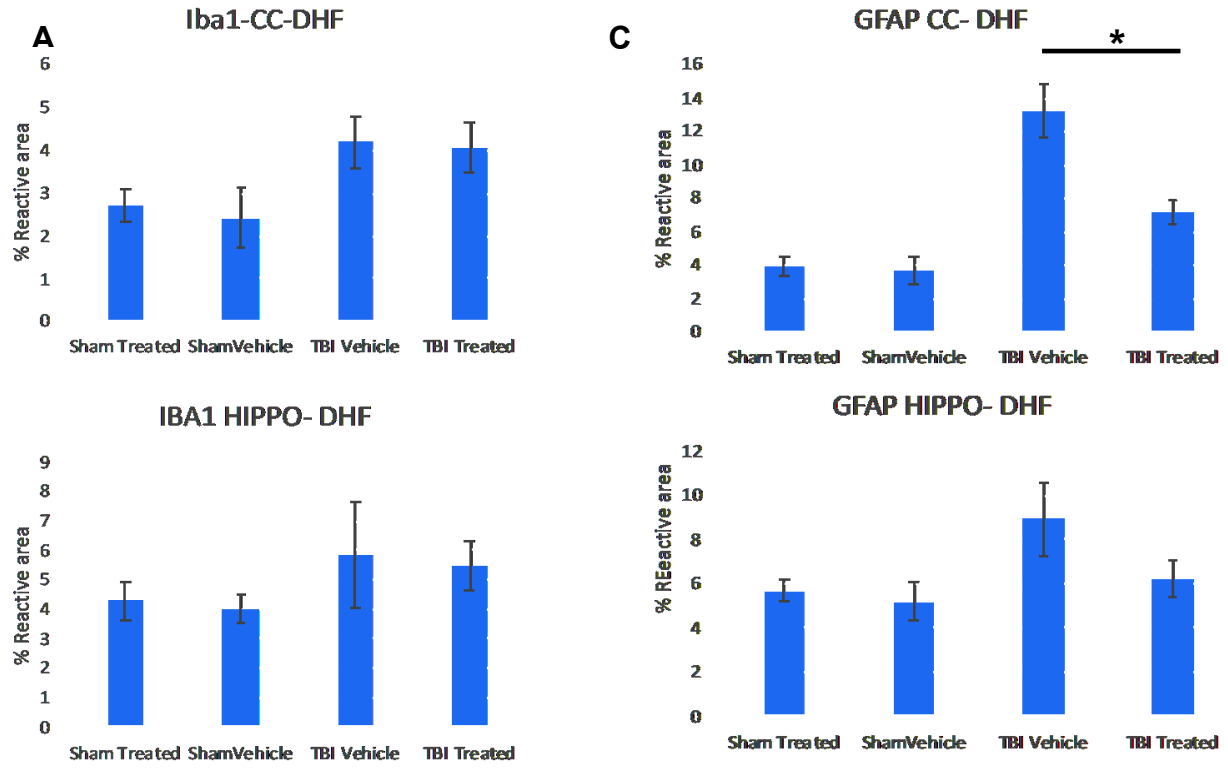

Figure 9: Microglia (IBA1) and astrocyte (GFAP) pathology in the hippocampus (HIPPO) and corpus callosum (CC) of a repetitive Mild Traumatic Brain Injury (r-mTBI) model after treatment with 7,8-Dihydroxyflavone (DHF). N=6/ per group. Asterisk denotes ***P<0.05***

Pharmacological blockade of Singosine-1-phosphate receptor after repetitive mTBI.

>Minimal effects of fingolimod on phospho-SIP1/SPHK1 levels post-injury. [Figure 10A-D]
>Fingolimod does not mitigate iNOS increase post-injury. [Figure 10E]
>Lack of effect on TBI-mediated astrogliosis and microgliosis, by fingolimod. [Figure 11]

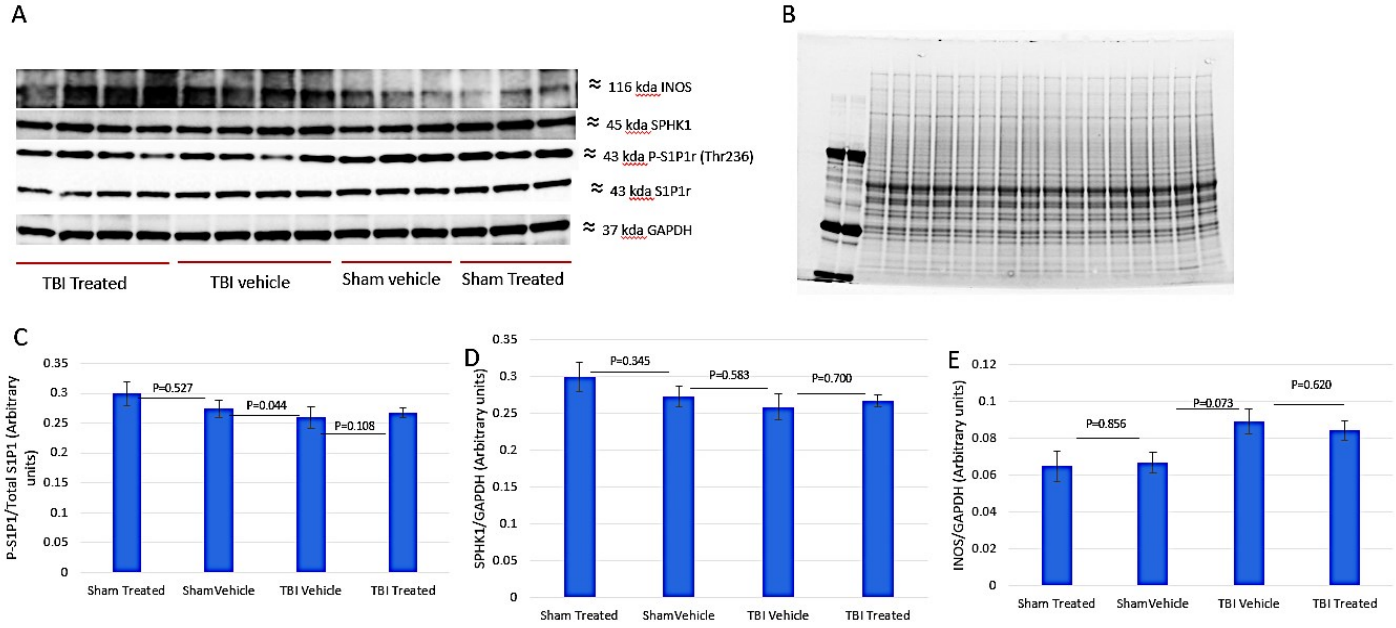

Figure.10. A) Immunoblot image showing representative results from cohort 4, Showing protein level expression of Sphingosine Kinase 1 (SPHK1),Phospho-sphingosine-1-phosphate receptor 1 (Thr236),Total Sphingosine-1-phosphate receptor 1, Inducible Nitric oxide synthase (INOS), and GAPDH (Housekeeping gene). B) Stain free image of gel electrophoresis used as a further normalization control. C) Graph showing Protein expression of Phospho-S1P1r / Total S1P1r. D) Graph showing protein expression of SPHK1. E) Graph showing protein expression of INOS. n=4 per group, error bars are shown as standard error of the mean (SEM) and data was statistically analyzed using a Students T-Test.

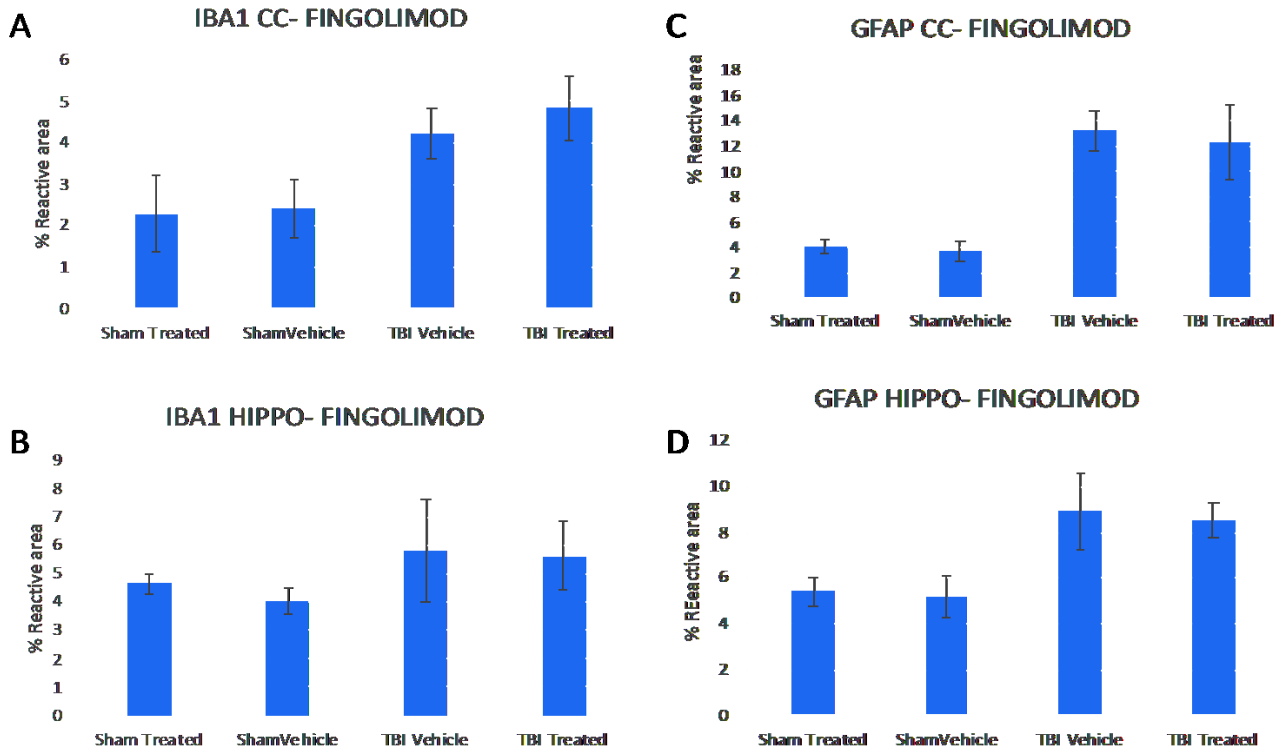

Figure 11: Microglia (IBA1) and astrocyte (GFAP) pathology in the hippocampus (HIPPO) and corpus callosum (CC) of a repetitive Mild Traumatic Brain Injury (r-mTBI) model after treatment with Fingolimod. N=6/ per group.

Pharmacological blockade of PPARγ receptor after repetitive mTBI.

>Significant increase in phospho-PPARγ signaling by pioglitazone following injury.

>Lack of mitigation of iNOS mediated increase post-injury, by pioglitazone.

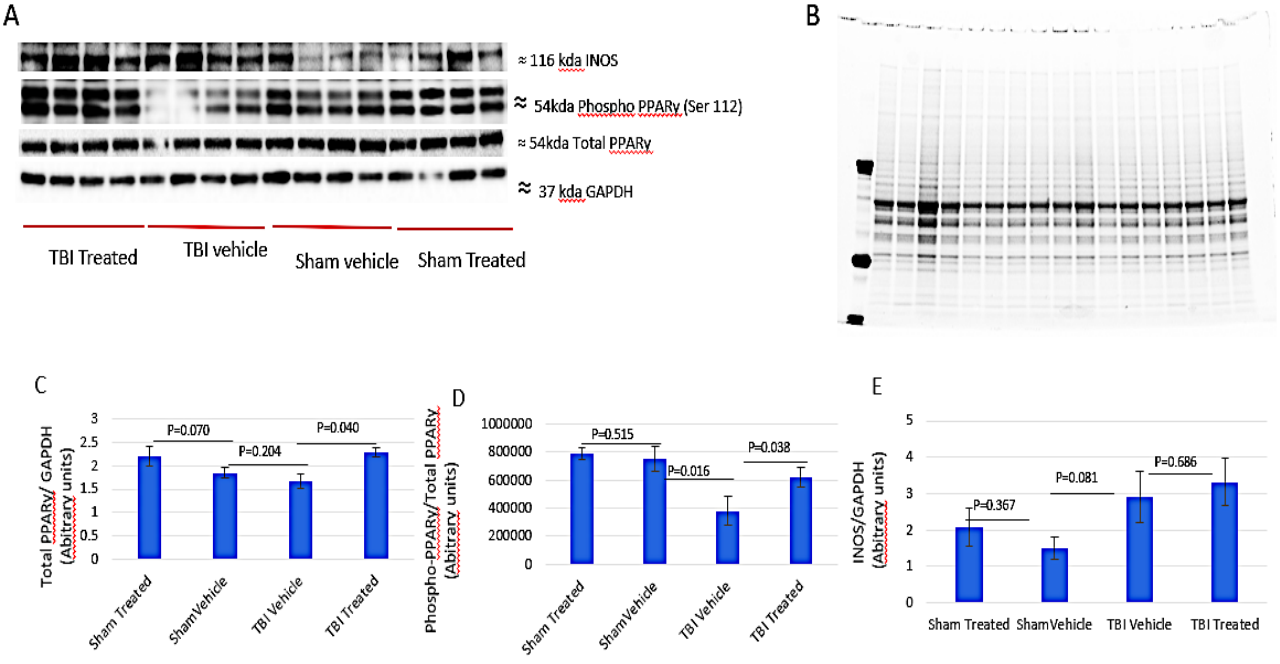

Figure.12. A) Immunoblot image showing representative results from cohort 5, Showing protein level expression of Peroxisome proliferator-activated receptor gamma (PPARγ), Phospho-Peroxisome proliferator-activated receptor gamma (PPARγ) Ser 112, Inducible Nitric oxide synthase (INOS), and GAPDH (Housekeeping gene). B) Stain free image of gel electrophoresis used as a further normalization control. C) Graph showing Protein expression of Total PPARγ. D) Graph showing protein expression of Phospho-PPARγ / Total PPARγ. E) Graph showing protein expression of INOS. n=4 per group, error bars are shown as standard error of the mean (SEM) and data was statistically analyzed using a Students T-Test.

Pharmacological blockade of IGF receptor after repetitive mTBI.

>Lack of significant increase in downstream IGF-signaling by intranasal insulin following injury.
>p-AKT ser473 shows a trend towards increase with intranasal insulin following injury.

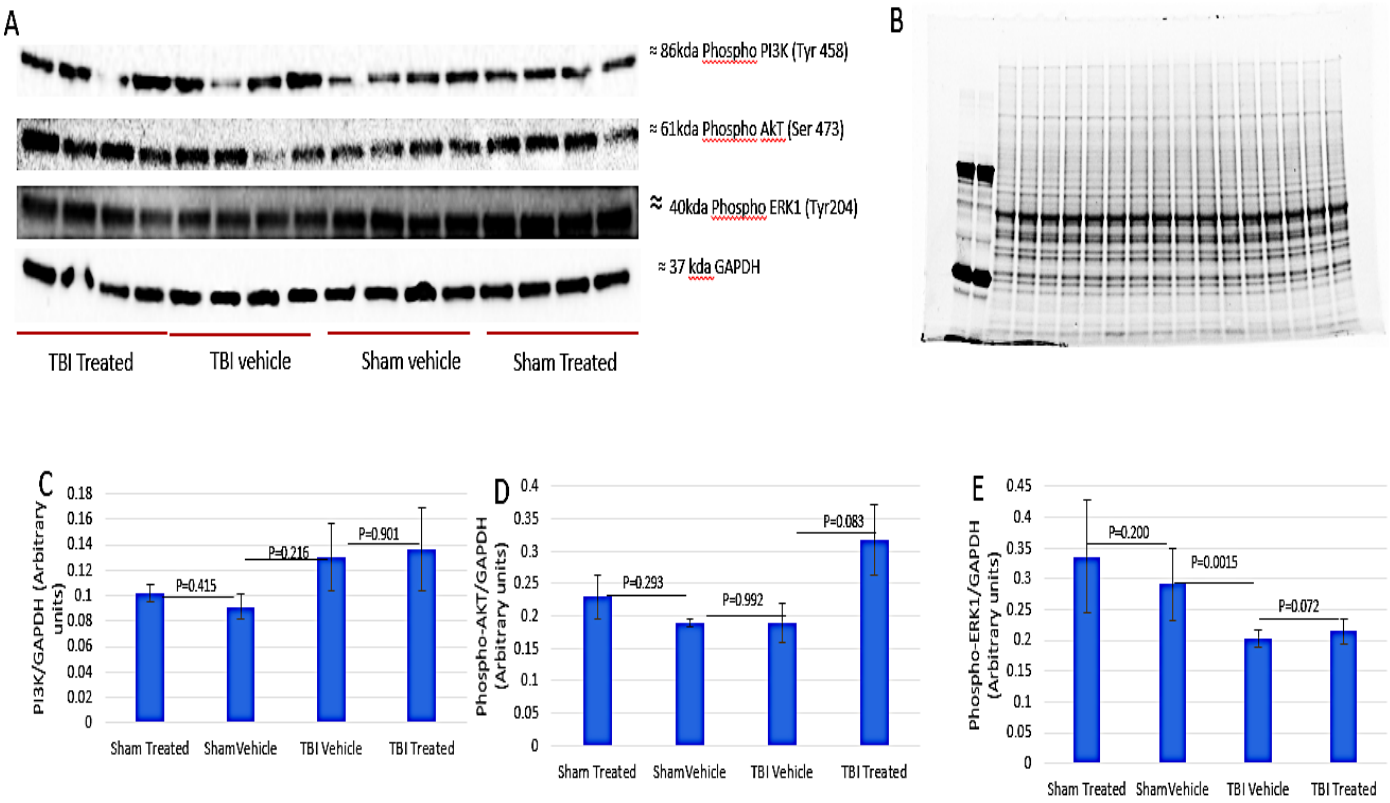

Figure.13. A) Immunoblot image showing representative results from cohort 6, Showing protein level expression of Phospho-Phosphoinositide 3-kinase(PI3K) Tyr458, Phospho-Protein kinase B (PKB), also known as Akt (P-AKT) Ser473, Phospho-Extracellular signal-regulated kinase1 (ERK1)and GAPDH (Housekeeping gene). B) Stain free image of gel electrophoresis used as a further normalization control. C) Graph showing Protein expression of PI3K when normalized for GAPDH. D) Graph showing protein expression of Phospho-AKT when normalized for GAPDH. E) Graph showing protein expression of Phospho-ERK1 when normalized for GAPDH. n=4 per group, error bars are shown as standard error of the mean (SEM) and data was statistically analyzed using a Students T-Test.

Bioactive lipid analysis of IMG microglia after LPS exposure, and treatment with Zileuton

Given the potent effects observed with Zileuton levels on microglia in our in vivo studies, we further explored the effects of Zileuton in a mouse immortalized microglia cell line after LPS stimulation. We first observed the bioactive lipid profiles following 2hrs after LPS stimulation to compare with brain profile changes in our previous lipidomic studies, and treated with Zileuton at 2, 4 and 6hrs post-injury. Potent effects were observed with Zileuton treatment on LTB4 and prostaglandins F2α levels at 4 and 6hrs post-LPS stimulation.

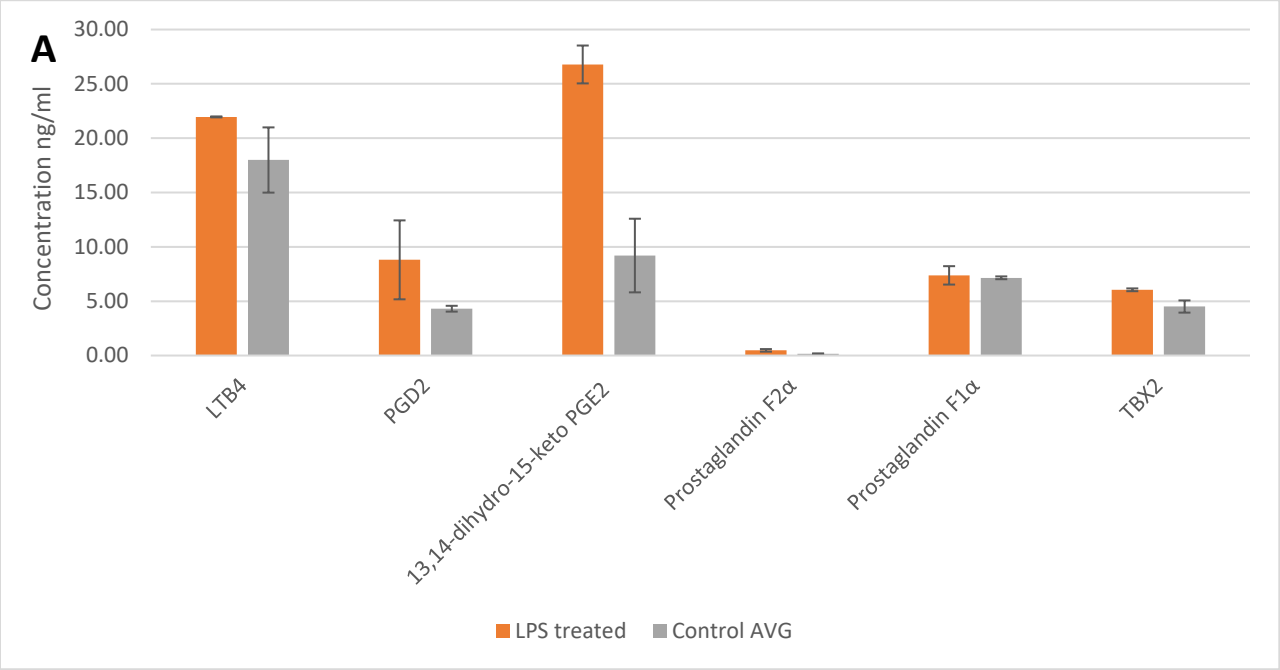

Figure. 14 .Bioactive lipid profile derived from LCMS/MS data showing the effect of 2 hours of 10ng/ml LPS administration on IMG microglia, LTB4= Leukotriene B4, PDG2= Prostaglandin D2,13,14-dihydro-15-keto prostaglandin E2, Prostaglandin F2a, Prostaglandin F1a and Thromboxane 2. n=2 per group, samples were run in triplicated error bars reported as Standard deviation.

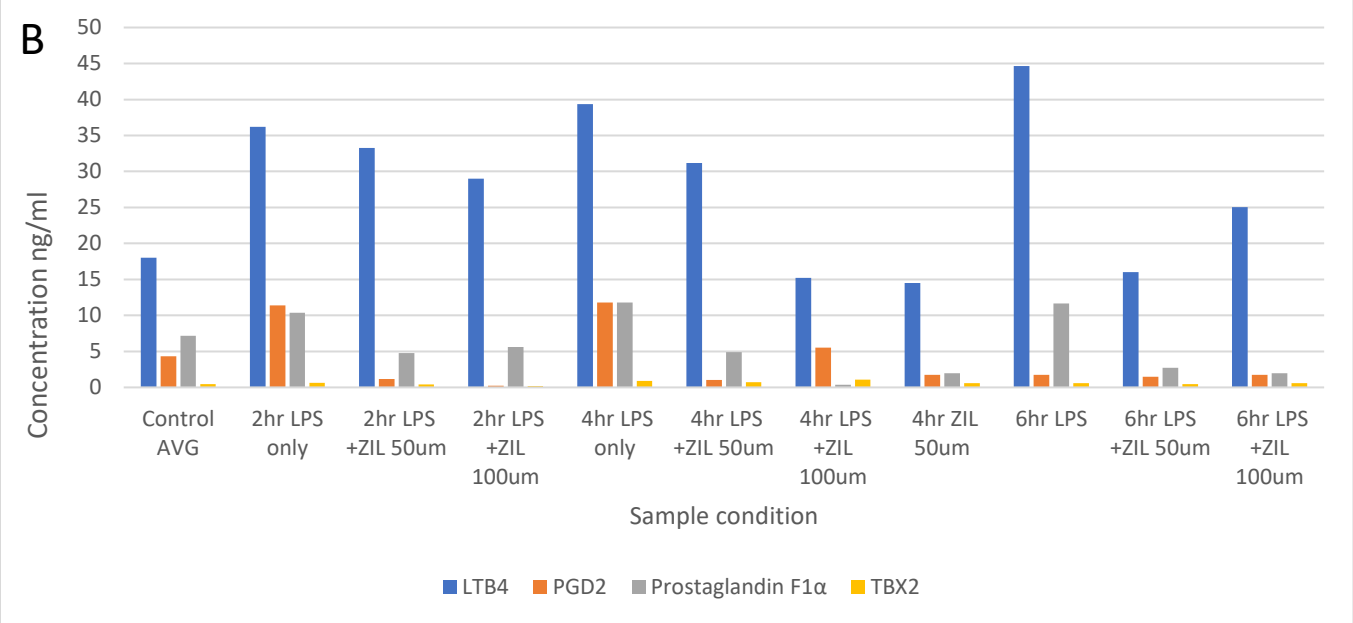

Figure. 15 .Bioactive lipid profile derived from LCMS/MS data showing the effect of 2,4 and 6 hours of 10ng/ml LPS administration on IMG microglia. Either with or without Zileuton (ZIL) @50 or 100uM LTB4= Leukotriene B4, PDG2= Prostaglandin D2, Prostaglandin F1a and Thromboxane 2. n=2 per group, samples were run in triplicated error bars reported as Standard deviation.

Neuroinflammatory profile of IMG microglia after LPS exposure (and in isolated adult microglial cells from our injury model)

Microglia cells play a prominent role in our injury model, and are attractive targets for mitigating TBI-mediated neurodegeneration in our model. Our previous drug compounds have shown potent effects on microglia activation states and underlying neuroinflammation in our injury paradigm. Thus, in anticipation of further single cell analyses of our drug compounds, we have generated time dependent profiles of iNOS, pNFkB, and COX-2 in immortalized microglial cell lines at different timepoints post-LPS/IFNγ treatment. We plan to screen potential drug targets from our in vivo work in these microglial cell lines treated with LPS or IFNγ in the next quarter. Results of these inflammatory protein profiles are shown below. We also plan to culture TBI-microglia vs sham-microglia to utilize as a screen of our drug compounds, and to interrogate isolated microglia cells from our injury paradigm after treatment.

iNOS, COX2, pNFkB levels from immortalized microglial cell lines after LPS simulation (2 and 24hrs)

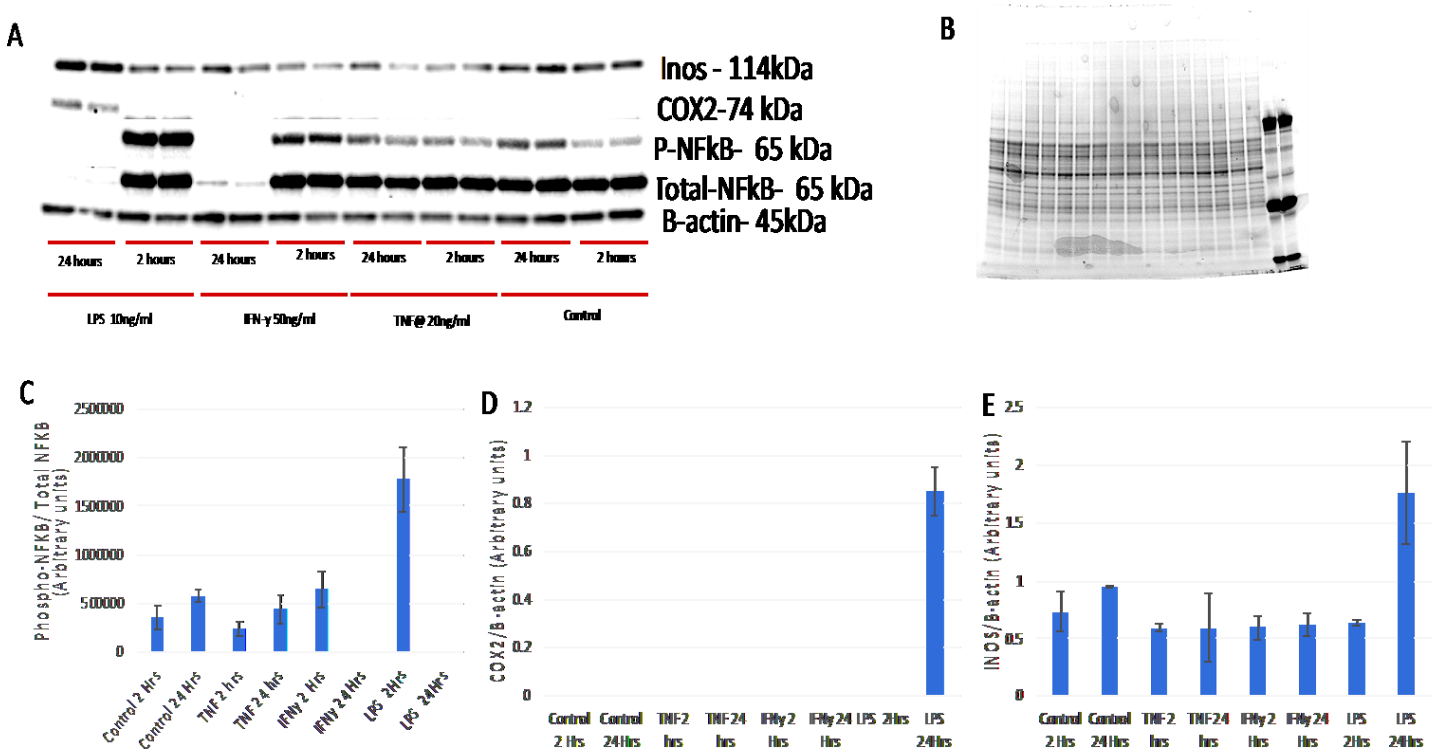

Figure.16. A) Immunoblot image showing representative results from IMG immortalized microglia when stimulated by either LPS @ 10ng/ml, TNFa @ 20ng/ml or IFN-y @ 50ng/ml for 2 or 24 hours, Showing protein level expression of Phospho-Nuclear Factor kappa Beta (NFkB) Ser536, Total Nuclear Factor kappa Beta (P65) ,Cyclooxygenase 2 (COX2), Inducible Nitric oxide synthase (INOS), and Beta-actin (Housekeeping gene). B) Stain free image of gel electrophoresis used as a further normalization control. C) Graph showing Protein expression of Phospho-NFkB/ Total NfkB when normalized for B-actin. D) Graph showing protein expression of COX2 when normalized for B-actin . E) Graph showing protein expression of INOS when normalized for B-actin. n=2 per group, error bars are shown as standard deviation.

iNOS, COX2, pNFkB levels from immortalized microglial cell lines after LPS simulation (15mins - 6hs)

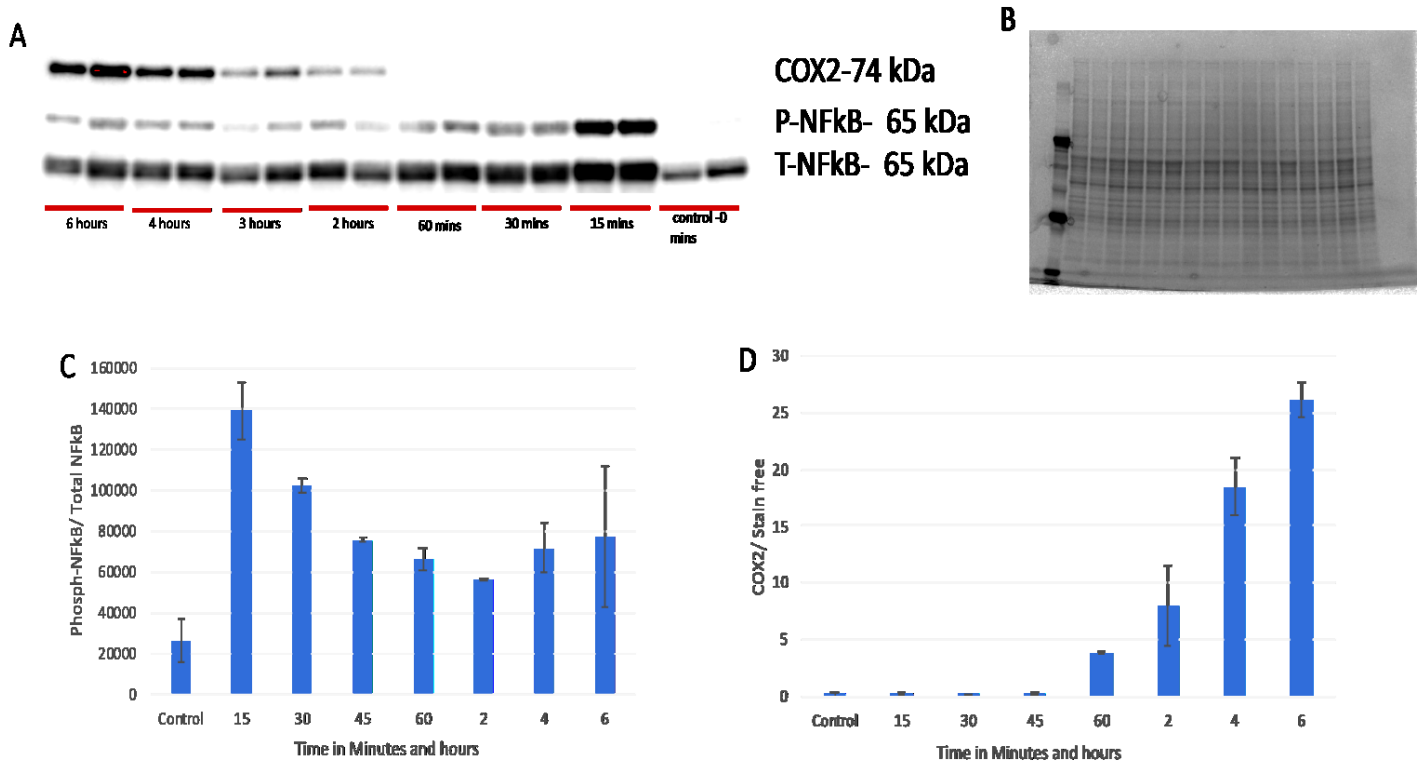

Figure.17. A) Immunoblot image showing representative results from IMG immortalized microglia when stimulated by LPS @ 10 ng/ml for between 15 minutes and 6 hours, Showing protein level expression of Phospho-Nuclear Factor kappa Beta (NFkB) Ser536, Total Nuclear Factor kappa Beta (P65) and Cyclooxygenase 2 (COX2). B) Stain free image of gel electrophoresis used as a normalization control. C) Graph showing Protein expression of Phospho-NFkB / Total NfkB when normalized for stain free. D) Graph showing protein expression of COX2 when normalized for stain free . n=2 per group, error bars are shown as standard deviation.

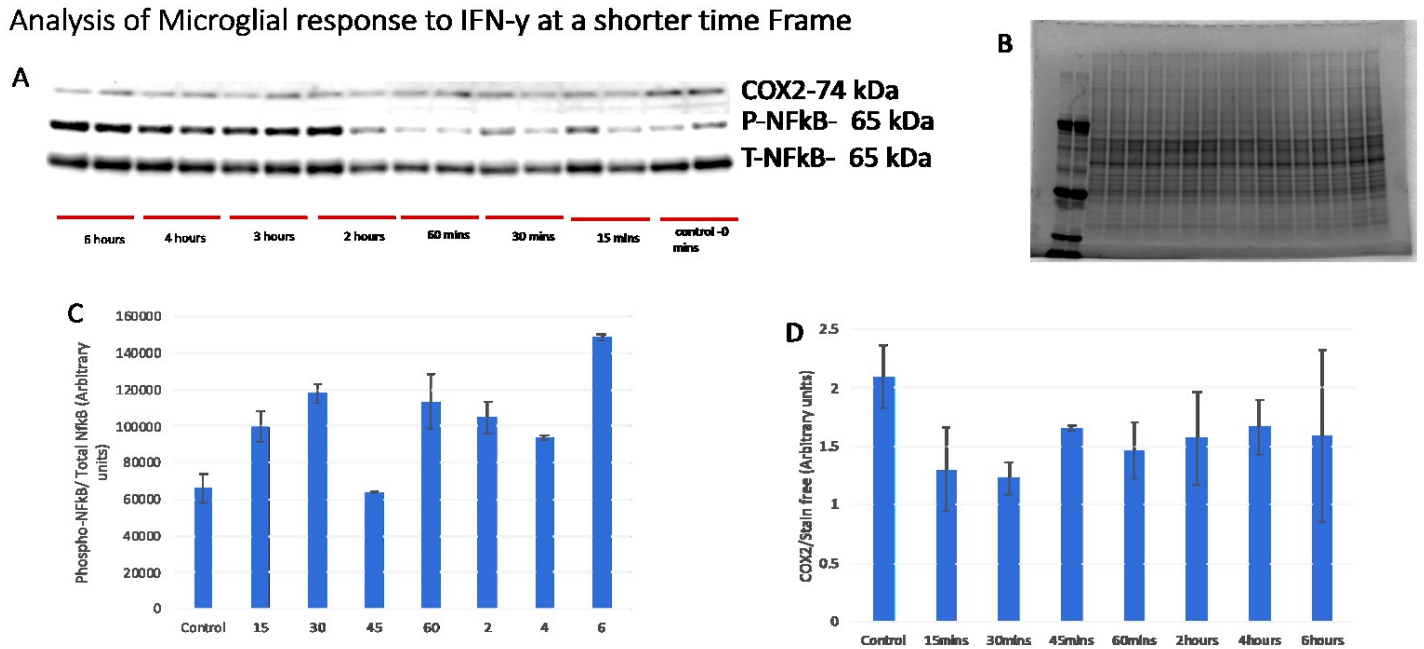

Figure.18. A) Immunoblot image showing representative results from IMG immortalized microglia when stimulated by IFN-Y @ 50 ng/ml for between 15 minutes and 6 hours, Showing protein level expression of Phospho-Nuclear Factor kappa Beta (NFkB) Ser536, Total Nuclear Factor kappa Beta (P65) and Cyclooxygenase 2 (COX2). B) Stain free image of gel electrophoresis used as a normalization control. C) Graph showing Protein expression of Phospho-NFkB / Total NfkB when normalized for stain free. D) Graph showing protein expression of COX2 when normalized for stain free . n=2 per group, error bars are shown as standard deviation.

Pharmacological blockade of TrkB receptor after repetitive mTBI

>No effect of 7,8-Dihydroxyflavone on microglia reactivity [Fig. 19A-E; 3A-E], but a significant effect is observed with astroglia activation post injury. [Fig. 20A-E; 4A-E]

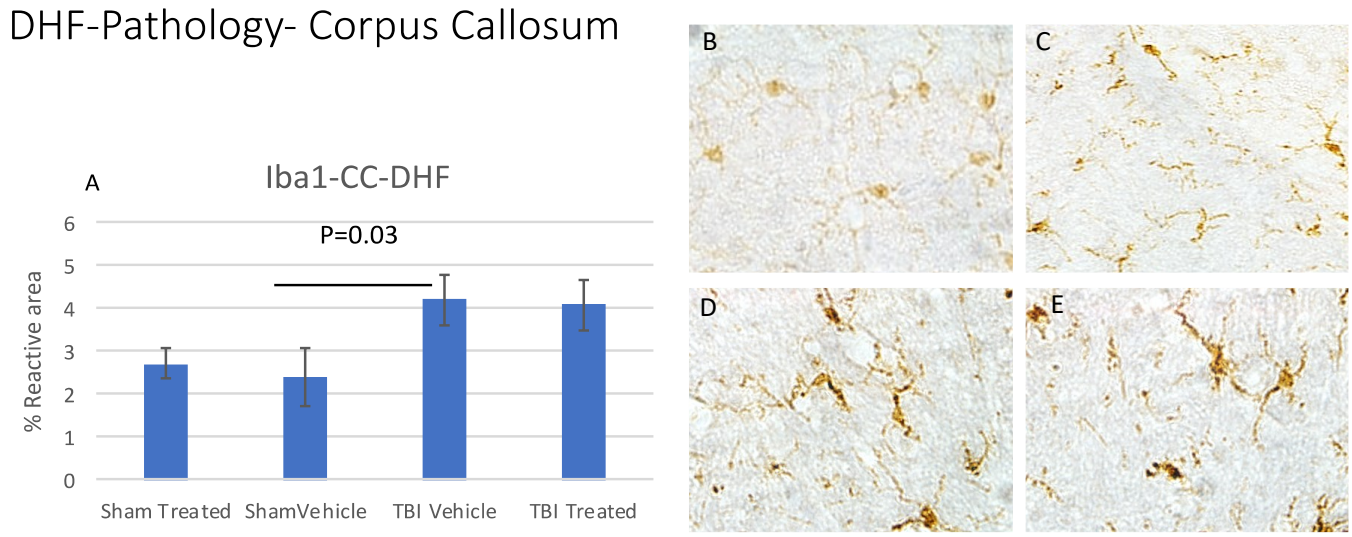

Figure 19: (A) Graph showing the % reactive area of Iba1 in the corpus callosum of sham or mTBI injured mice who either received vehicle or treatment with 7'8-DHF. Error bars represent SEM. (B) Representative image of the corpus Callosum of sham vehicle mice for Iba1. (C) Representative image of the corpus Callosum of sham Treated mice for Iba1. (D) Representative image of the corpus Callosum of TBI vehicle mice for Iba1. (E) Representative image of the corpus Callosum of TBI Treated mice for Iba1.

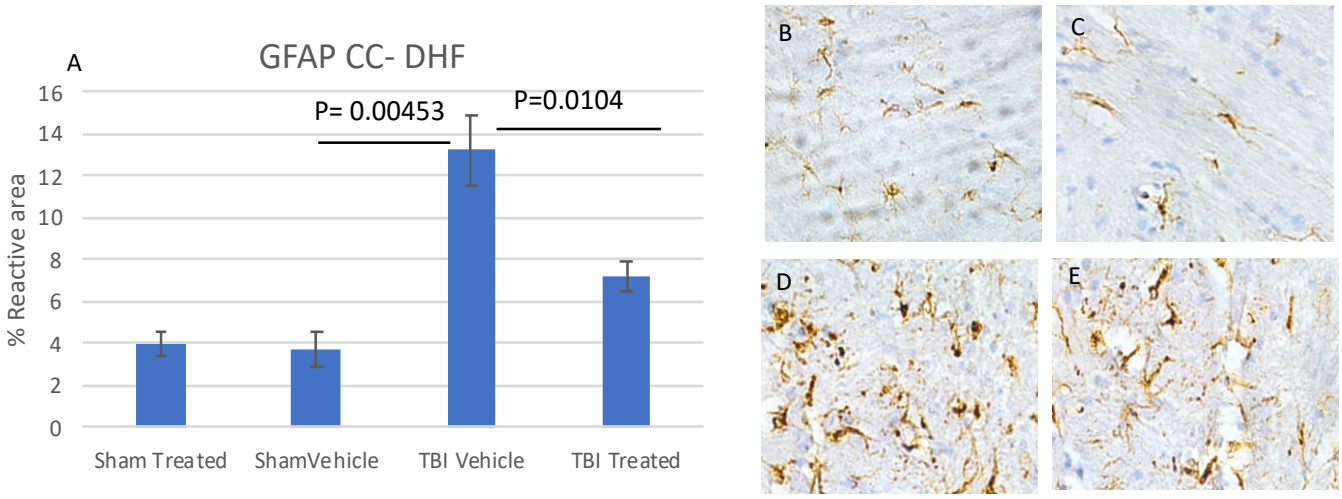

Figure 20: (A) Graph showing the % reactive area of GFAP in the corpus callosum of sham or mTBI injured mice who either received vehicle or treatment with 7'8-DHF. Error bars represent SEM. (B) Representative image of the corpus Callosum of sham vehicle mice for GFAP. (C) Representative image of the corpus Callosum of sham Treated mice for GFAP. (D) Representative image of the corpus Callosum of TBI vehicle mice for GFAP. (E) Representative image of the corpus Callosum of TBI Treated mice for GFAP.

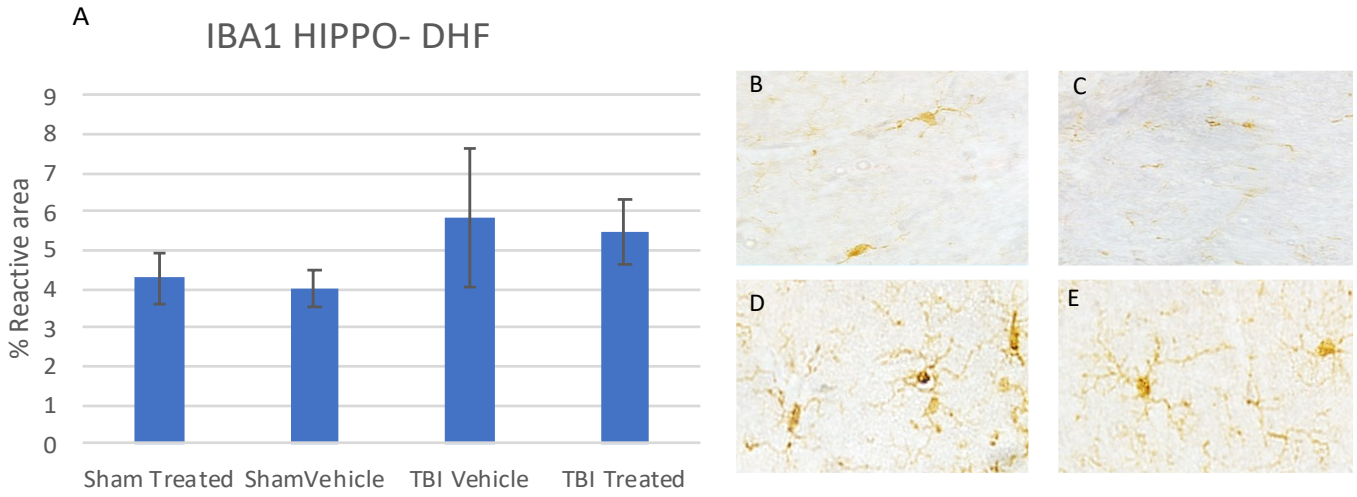

Figure 21: (A) Graph showing the % reactive area of Iba1 in the Hippocampus of sham or mTBI injured mice who either received vehicle or treatment with 7'8-DHF. Error bars represent SEM. (B) Representative image of the Hippocampus of sham vehicle mice for Iba1. (C) Representative image of the Hippocampus of sham Treated mice for Iba1. (D) Representative image of the Hippocampus of TBI vehicle mice for Iba1. (E) Representative image of the Hippocampus of TBI Treated mice for Iba1.

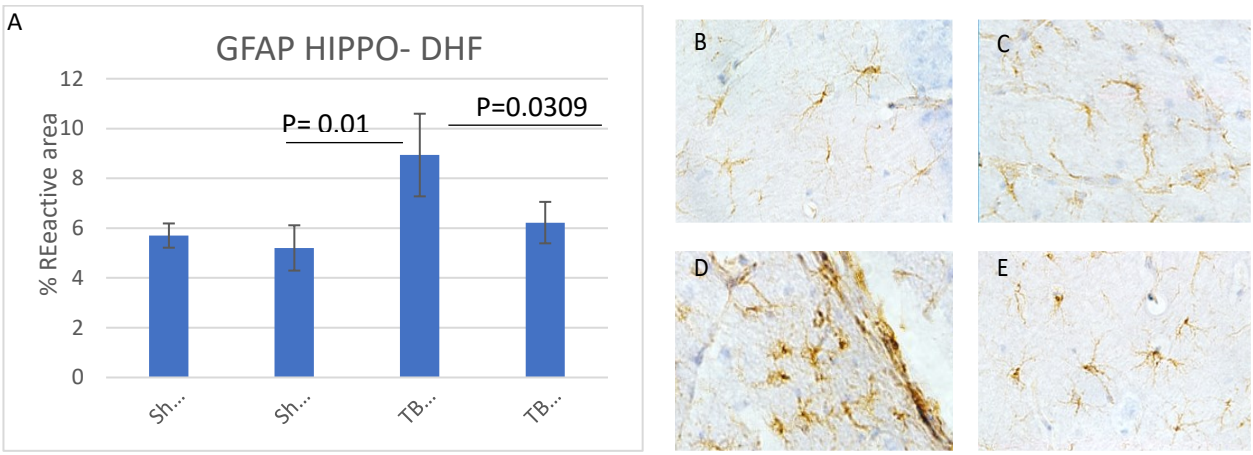

Figure 22: (A) Graph showing the % reactive area of GFAP in the Hippocampus of sham or mTBI injured mice who either received vehicle or treatment with 7'8-DHF. Error bars represent SEM. (B) Representative image of the Hippocampus of sham vehicle mice for GFAP. (C) Representative image of the Hippocampus of sham Treated mice for GFAP. (D) Representative image of the Hippocampus of TBI vehicle mice for GFAP. (E) Representative image of the Hippocampus of TBI Treated mice for GFAP.

Pharmacological blockade of Singosine-1-phosphate receptor after repetitive mTBI.

No effect of fingolimod on astroglia or microglia activation post-injury. [see Figure 23-26]

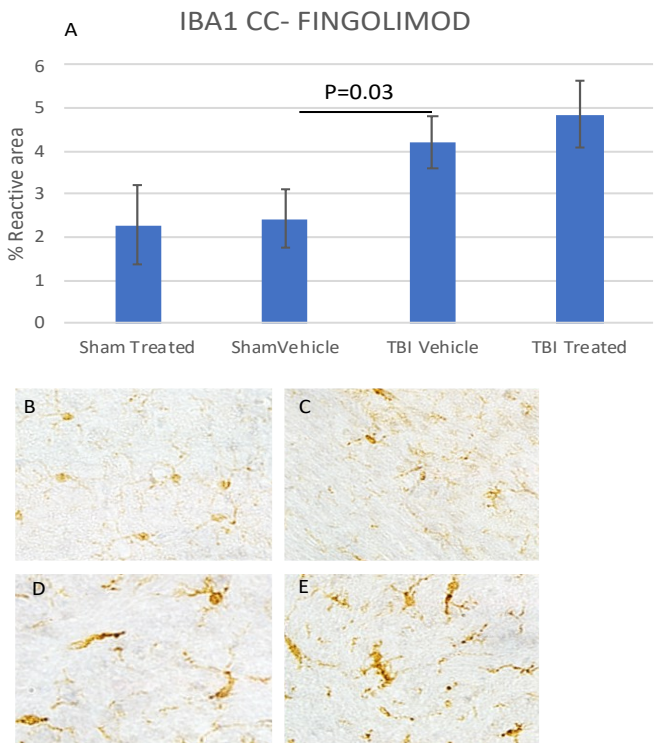

Figure 23 (A) Graph showing the % reactive area of Iba1 in the corpus callosum of sham or mTBI injured mice who either received vehicle or treatment with Fingolimod. Error bars represent SEM. (B)Representative image of the corpus Callosum of sham vehicle mice for Iba1. (C)Representative image of the corpus Callosum of sham Treated mice for Iba1. (D) Representative image of the corpus Callosum of TBI vehicle mice for Iba1. (E) Representative image of the corpus Callosum of TBI Treated mice for

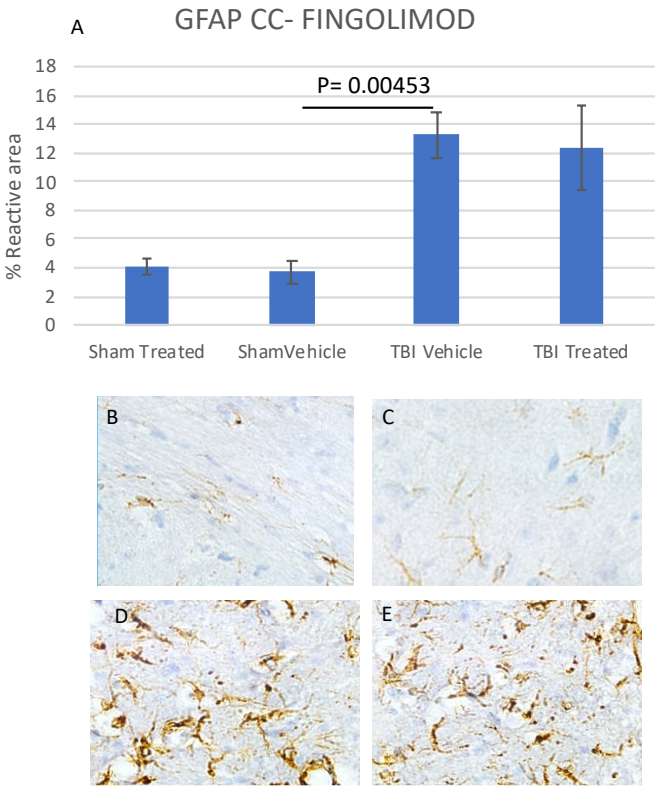

Figure 24 (A)Graph showing the % reactive area of GFAP in the corpus callosum of sham or mTBI injured mice who either received vehicle or treatment with Fingolimod. Error bars represent SEM. (B)Representative image of the corpus Callosum of sham vehicle mice for GFAP. (C)Representative image of the corpus Callosum of sham Treated mice for GFAP. (D) Representative image of the corpus Callosum of TBI vehicle mice for GFAP. (E) Representative image of the corpus Callosum of TBI Treated mice for GFAP.

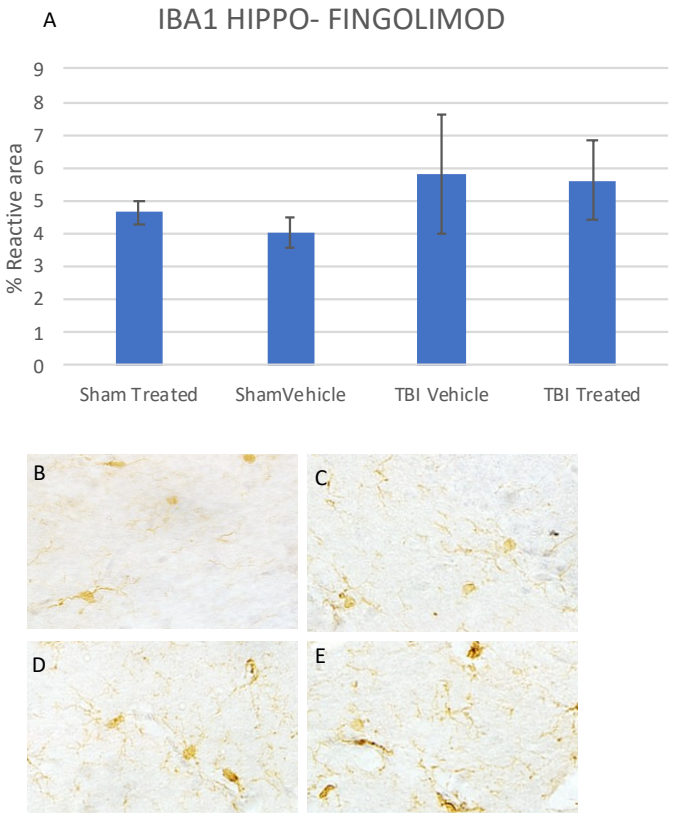

Figure 25 (A)Graph showing the % reactive area of Iba1 in the Hippocampus of sham or mTBI injured mice who either received vehicle or treatment with Fingolimod. Error bars represent SEM. (B)Representative image of the Hippocampus of sham vehicle mice for Iba1. (C)Representative image of the Hippocampus of sham Treated mice for Iba1. (D) Representative image of the Hippocampus of TBI vehicle mice for Iba1. (E) Representative image of the Hippocampus of TBI Treated mice for Iba1.

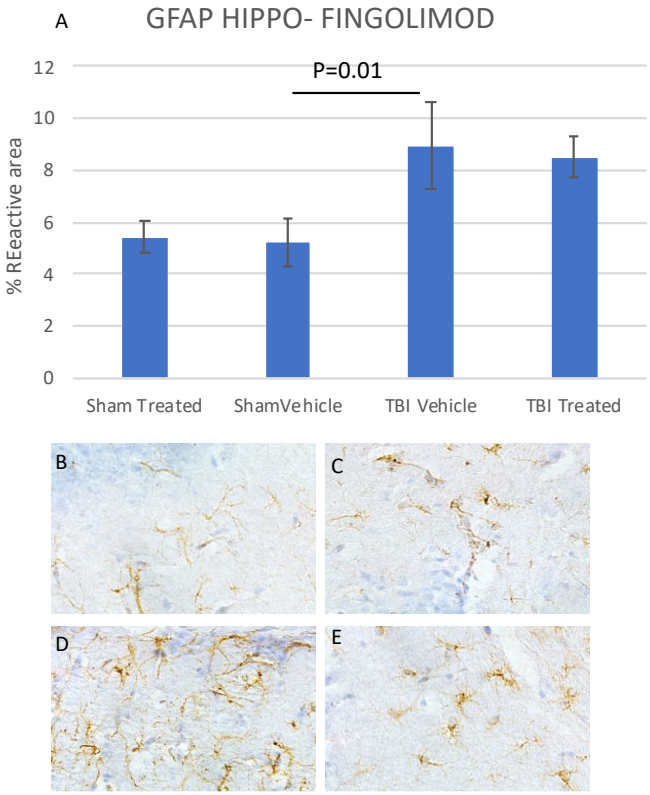

Figure 26: (A) Graph showing the % reactive area of GFAP in the Hippocampus of sham or mTBI injured mice who either received vehicle or treatment with Fingolimod. Error bars represent SEM. (B)Representative image of the Hippocampus of sham vehicle mice for GFAP. (C)Representative image of the Hippocampus of sham Treated mice for GFAP. (D) Representative image of the Hippocampus of TBI vehicle mice for GFAP. (E) Representative image of the Hippocampus of TBI Treated mice for GFAP.

Pharmacological blockade of PPARγ receptor after repetitive mTBI.

>Mitigates glial activation in the corpus callosum (Figure 27 and 28).

>Mitigates astroglia activation in the hippocampus (Figure 30), but no change was observed in microglia activation in the hippocampus (Figure 29).

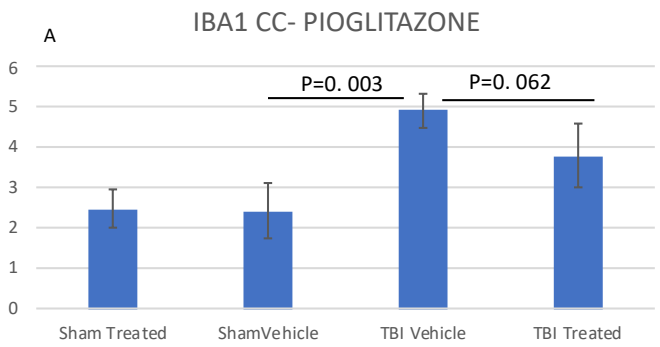

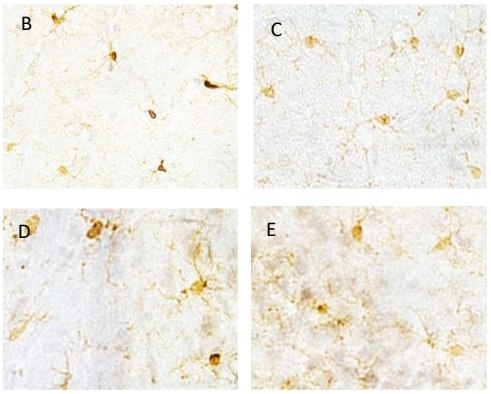

Figure 27: (A)Graph showing the % reactive area of Iba1 in the corpus callosum of sham or mTBI injured mice who either received vehicle or treatment with Pioglitazone. Error bars represent SEM. (B)Representative image of the corpus Callosum of sham vehicle mice for Iba1. (C)Representative image of the corpus Callosum of sham Treated mice for Iba1. (D) Representative image of the corpus Callosum of TBI vehicle mice for Iba1. (E) Representative image of the corpus Callosum of TBI Treated mice for Iba1.

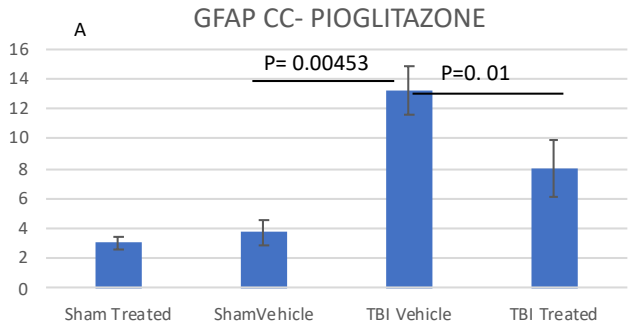

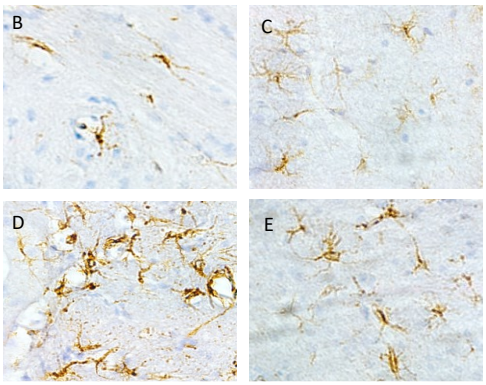

Figure 28: (A)Graph showing the % reactive area of GFAP in the corpus callosum of sham or mTBI injured mice who either received vehicle or treatment with Pioglitazone. Error bars represent SEM. (B)Representative image of the corpus Callosum of sham vehicle mice for GFAP. (C)Representative image of the corpus Callosum of sham Treated mice for GFAP. (D) Representative image of the corpus Callosum of TBI vehicle mice for GFAP. (E) Representative image of the corpus Callosum of TBI Treated mice for GFAP.

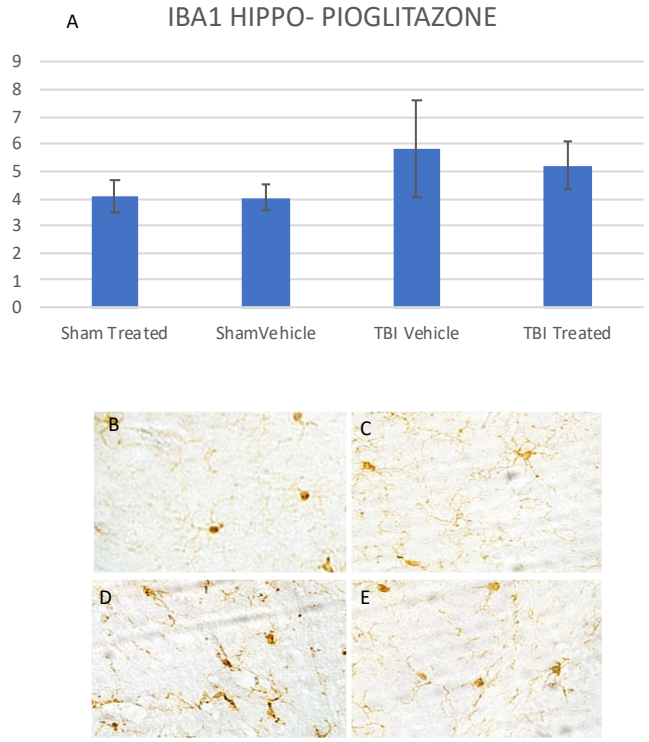

Figure 29: (A) Graph showing the % reactive area of Iba1 in the Hippocampus of sham or mTBI injured mice who either received vehicle or treatment with Pioglitazone. Error bars represent SEM. (B)Representative image of the Hippocampus of sham vehicle mice for Iba1. (C)Representative image of the Hippocampus of sham Treated mice for Iba1. (D) Representative image of the Hippocampus of TBI vehicle mice for Iba1. (E) Representative image of the Hippocampus of TBI Treated mice for Iba1.

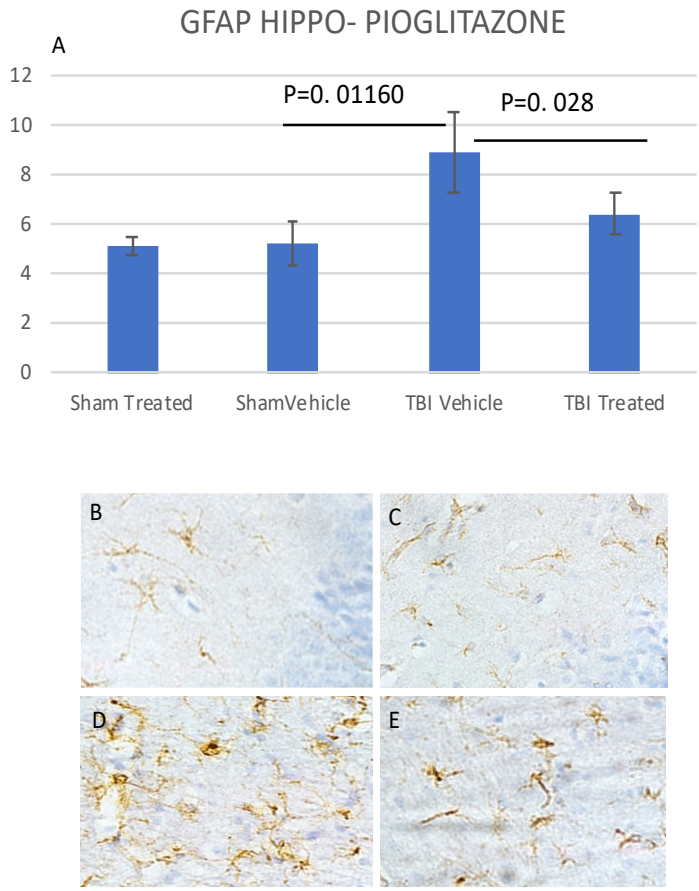

Figure 30: (A)Graph showing the % reactive area of GFAP in the Hippocampus of sham or mTBI injured mice who either received vehicle or treatment with Pioglitazone. Error bars represent SEM. (B)Representative image of the Hippocampus of sham vehicle mice for GFAP. (C)Representative image of the Hippocampus of sham Treated mice for GFAP. (D) Representative image of the Hippocampus of TBI vehicle mice for GFAP. (E) Representative image of the Hippocampus of TBI Treated mice for GFAP.

Pharmacological blockade of IGF receptor after repetitive mTBI.

>No change in glial activation was observed with this treatment in the hippocampus or corpus callosum after injury (Figure 31-34).

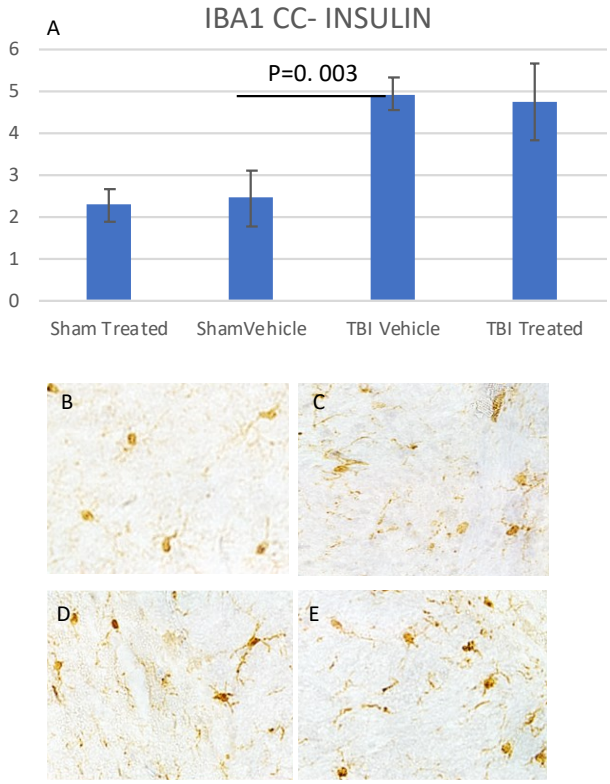

Figure 31: (A) Graph showing the % reactive area of Iba1 in the corpus callosum of sham or mTBI injured mice who either received vehicle or treatment with Insulin. Error bars represent SEM. (B) Representative image of the corpus Callosum of sham vehicle mice for Iba1. (C) Representative image of the corpus Callosum of sham Treated mice for Iba1. (D) Representative image of the corpus Callosum of TBI vehicle mice for Iba1. (E) Representative image of the corpus Callosum of TBI Treated mice for Iba1.

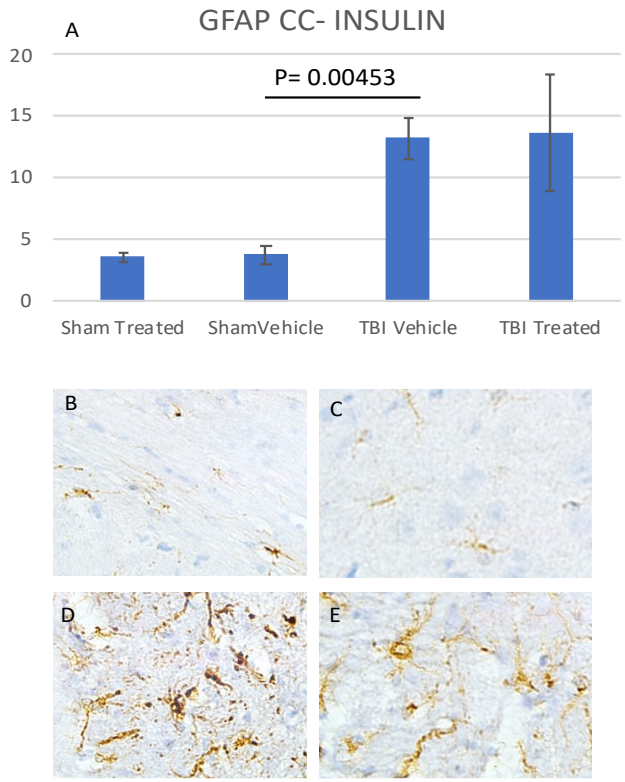

Figure 32: (A) Graph showing the % reactive area of GFAP in the corpus callosum of sham or mTBI injured mice who either received vehicle or treatment with Insulin. Error bars represent SEM. (B) Representative image of the corpus Callosum of sham vehicle mice for GFAP. (C) Representative image of the corpus Callosum of sham Treated mice for GFAP. (D) Representative image of the corpus Callosum of TBI vehicle mice for GFAP. (E) Representative image of the corpus Callosum of TBI Treated mice for GFAP.

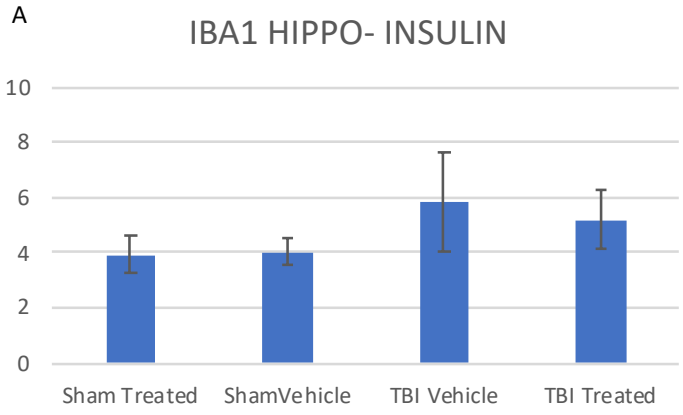

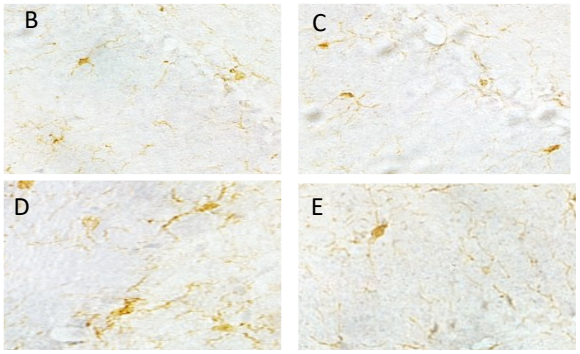

Figure 33: (A) Graph showing the % reactive area of Iba1 in the Hippocampus of sham or mTBI injured mice who either received vehicle or treatment with Insulin. Error bars represent SEM. (B) Representative image of the Hippocampus of sham vehicle mice for Iba1. (C)Representative image of the Hippocampus of sham Treated mice for Iba1. (D) Representative image of the Hippocampus of TBI vehicle mice for Iba1. (E) Representative image of the Hippocampus of TBI Treated mice for Iba1.

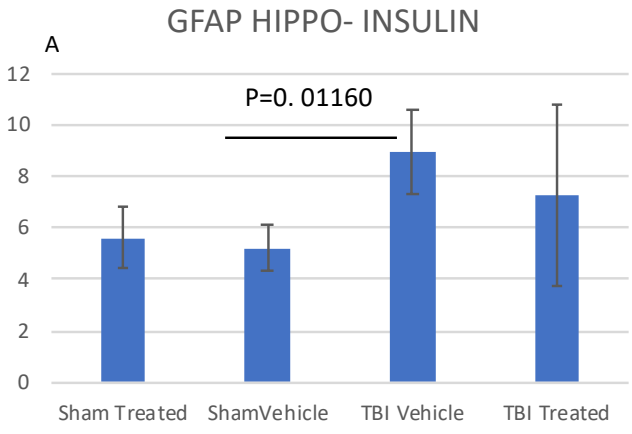

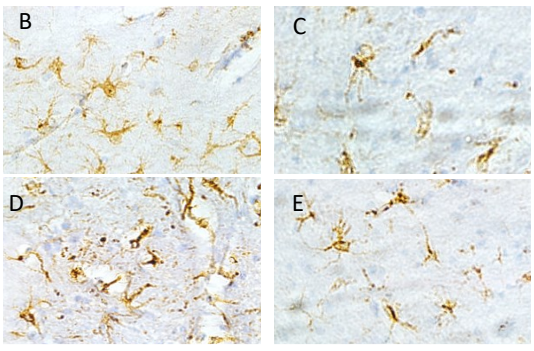

Figure 34: (A) Graph showing the % reactive area of GFAP in the Hippocampus of sham or mTBI injured mice who either received vehicle or treatment with Insulin. Error bars represent SEM. (B) Representative image of the Hippocampus of sham vehicle mice for GFAP. (C) Representative image of the Hippocampus of sham Treated mice for GFAP. (D) Representative image of the Hippocampus of TBI vehicle mice for GFAP. (E) Representative image of the Hippocampus of TBI Treated mice for GFAP.

Target Engagement: Changes in Phospho- C-KIT (receptor tyrosine kinase) following Injury and treatment with Montelukast (Cysteinyl leukotriene receptor)

>phospho-C-KIT (TYR703) – Figure 35

>phospho-ERK1/2 (Thre202/Tyr204) – Figure 36

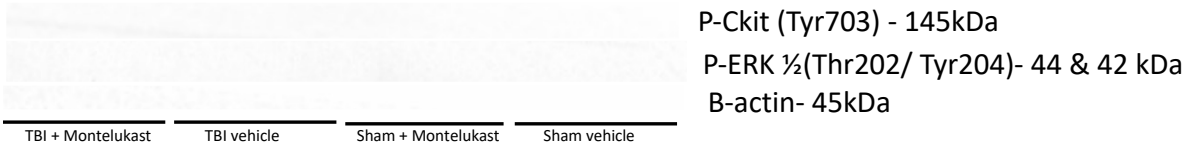

P-Ckit (Tyr703) - 145kDa

P-ERK ½(Thr202/ Tyr204)- 44 & 42 kDa

B-actin- 45kDa

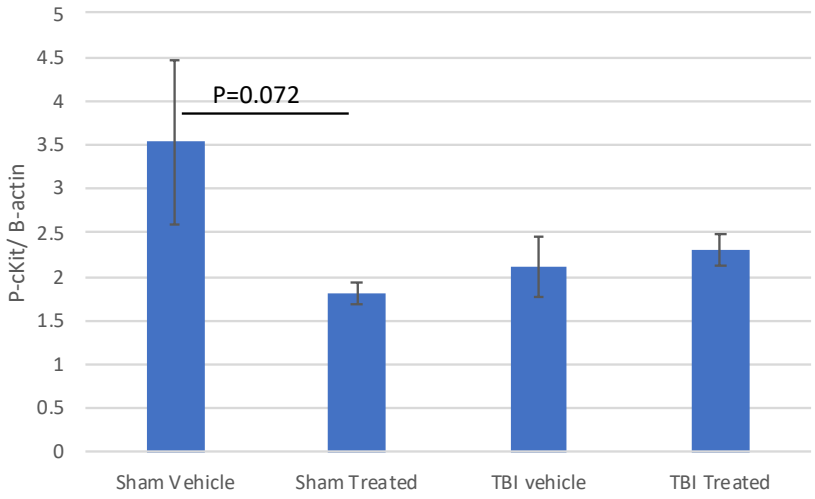

Figure 35: A graph showing the protein expression of Phospho C-KIT (TYR703) in mouse brain homogenate, data were normalized to B-actin, data were assessed using a students T tests. Sham vehicle (n=4) vs TBI- vehicle (n=4) P= 0.199 , TBI- vehicle (n=4) vs TBI + Montelukast (n=4) P= 0.616. Sham vehicle vs Sham + Montelukast P= 0.072. Error bars represent SEM.

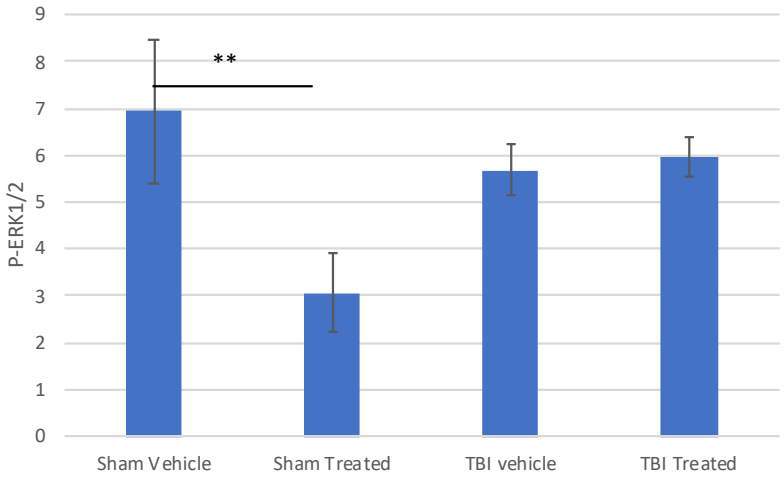

*Figure 36: A graph showing the protein expression of Phospho ERK1/2 (Thr202/ Tyr204)- in mouse brain homogenate, data were normalized to B-actin, data were assessed using a students T tests. Sham vehicle (n=4) vs TBI- vehicle (n=4) P= 0.499 , TBI- vehicle (n=4) vs TBI + Montelukast (n=4) P= 0.722. . Sham vehicle vs Sham + Montelukast P= 0.0038 (Indicated by **) Error bars represent SEM.*

Validation of Top performing compound targets (to date) in human tissue

>phospho-PPARgamma (ser112) – Figure 37
>phospho-5-LOX (ser663) – Figure 36

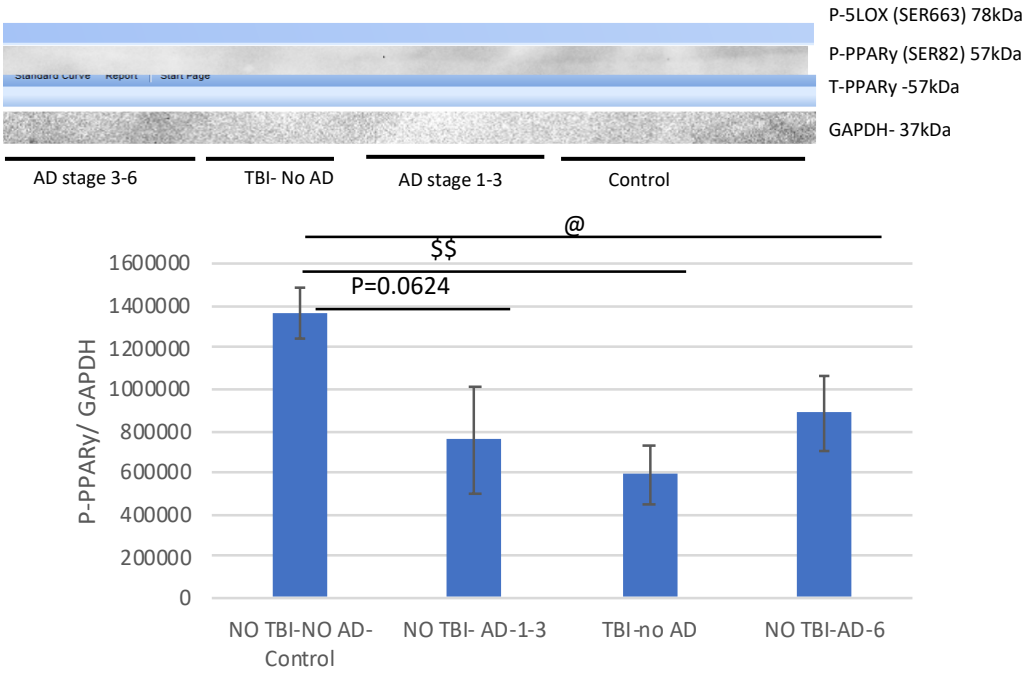

Figure 37: *graph showing the protein expression of Phospho- PPARY (Serine 112) in the cytoplasmic fraction of human medial temporal lobe homogenate, data were normalized to Total PPARY and to GAPDH, data were assessed using a students T tests. Control (n=10) vs AD(1-3) no TBI (n=6) P= 0.0624 , Control (n=10) vs TB No AD (n=3) P= 0.0034332 (Indicated by $$). Control (n=10) vs AD(3-6) (n=9) P= 0.0112(Indicated by @). Error bars represent SEM.*

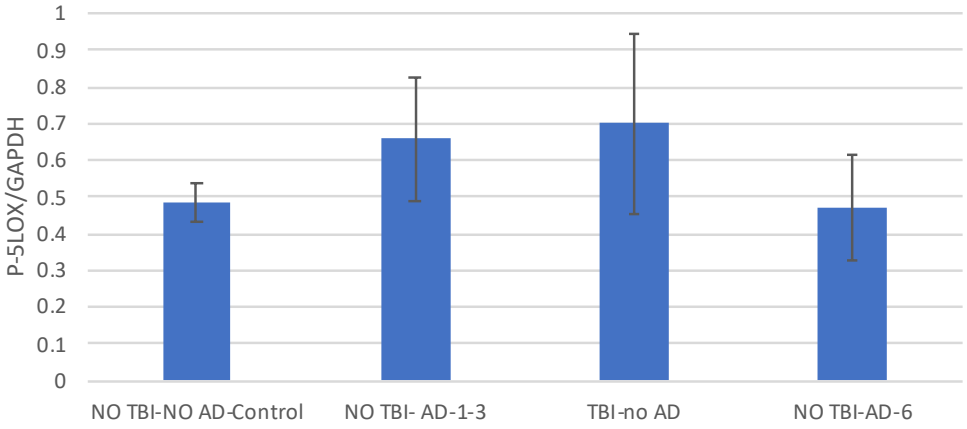

Figure 38: *A graph showing the protein expression of Phospho-5LOX (Serine 663) in the cytoplasmic fraction of human medial temporal lobe homogenate, data were normalized to Total 5-LOX and to GAPDH, data were assessed using a students T tests. Control (n=10) vs AD(1-3) no TBI (n=6) P= 0.324 , Control (n=10) vs TB No AD (n=3) P= 0.7863. Control (n=10) vs AD(3-6) (n=9) P= 0.477. Error bars represent SEM.*

Lipidomic analysis of Isolated glia from TBI and sham mice (Pilot study for future target engagement assessment for studies in Task 2)

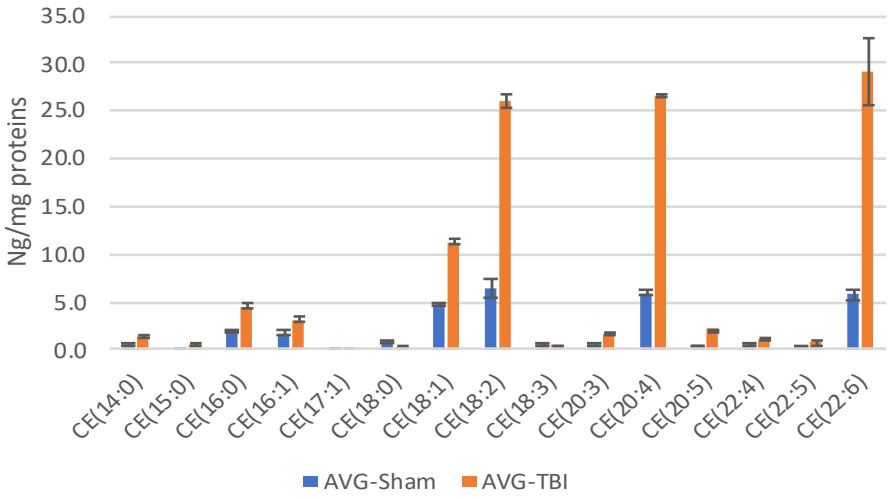

Figure 39: A graph showing the abundance of cholesterol esters in isolated mixed glial cells from sham and Injured mice (n= 2/ group). Error bars show the SEM.

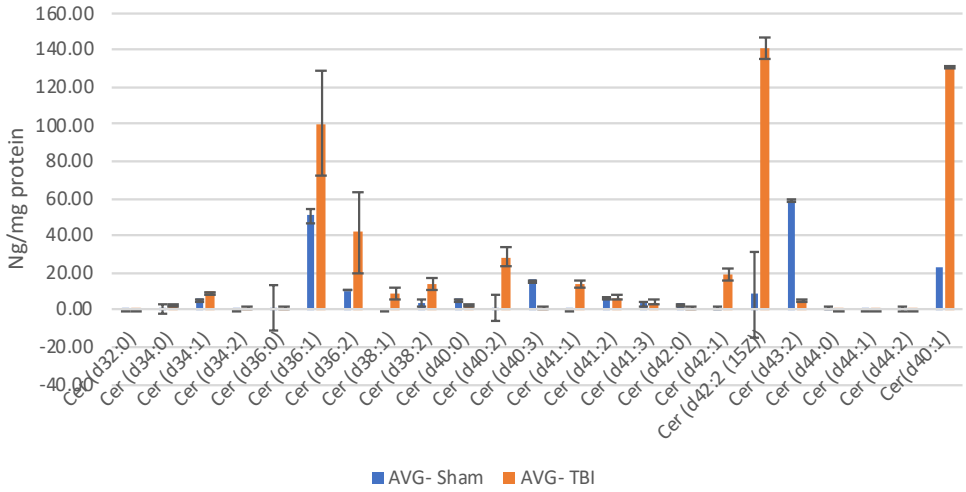

Figure 40: A graph showing the abundance of ceramides in isolated mixed glial cells from sham and Injured mice (n= 2/ group). Error bars show the SEM.

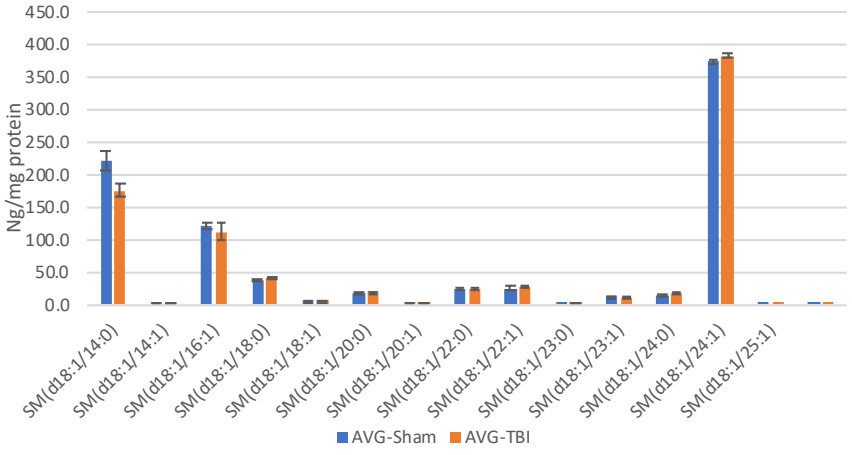

Figure 41: A graph showing the abundance of Sphingomyelin based sphingolipids in isolated mixed glial cells from sham and Injured mice (n= 2/ group). Error bars show the SEM.

Evaluation of effects on iNos, pSTAT3, p5LOX, pNFKB, pPPARg (Figure 42A-E) in isolated glial cells after *in vivo* exposure to Top two performing drugs in our mild (5hit) r-sham/r-mTBI model.

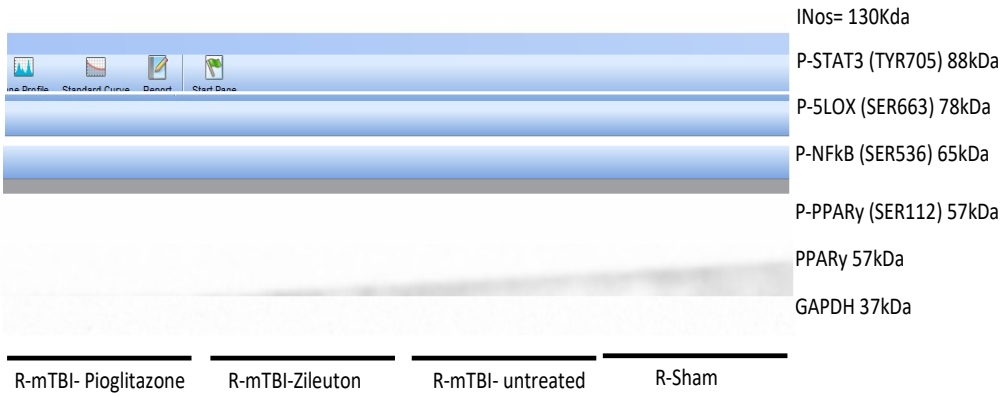

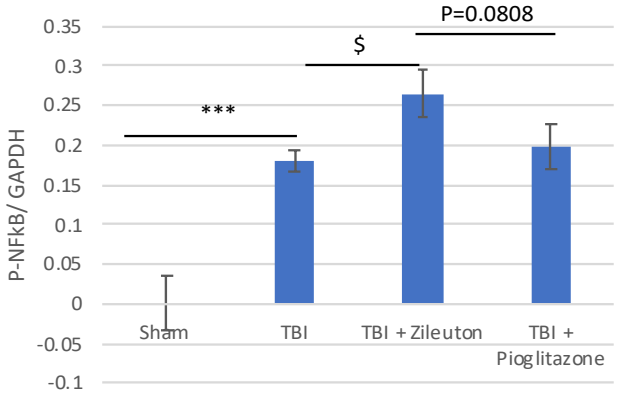

*Figure 42A: A graph showing the protein expression of Phospho-NFkB (Serine 536) in isolated mixed glial cells, data were normalized to Total NFkB (not shown) and to GAPDH, data were assessed using a students T tests. Sham (n=4) vs TBI- untreated (n=4) P= 0.006 (indicated by ***), TBI- untreated (n=4 vs TBI + Zileuton (n=4) P= 0.0210 (Indicated by $). TBI- untreated (n=4 vs TBI + Pioglitazone (n=4) P= 0.283. TBI + Zileuton (n=4) vs TBI + Pioglitazone (n=4) P= 0.0808. Error bars represent SEM.*

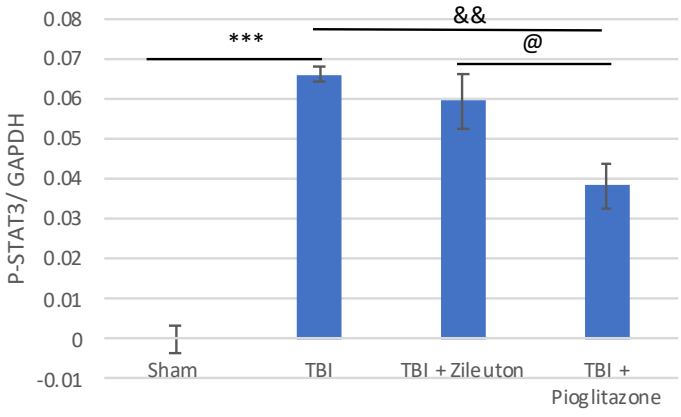

*Figure 42B: A graph showing the protein expression of Phospho-STAT3 (Tyrosine705) in isolated mixed glial cells, data were normalized to Total STAT3 (not shown) and to GAPDH, data were assessed using a students T tests. Sham (n=4) vs TBI- untreated (n=4) P= 0.0002 (indicated by ***), TBI- untreated (n=4 vs TBI + Zileuton (n=4) P=0.187. TBI- untreated (n=4) vs TBI + Pioglitazone (n=4) P= 0.0019 (indicated by &&). TBI + Zileuton (n=4) vs TBI + Pioglitazone (n=4) P= 0.027 (indicated by @). Error bars represent SEM.*

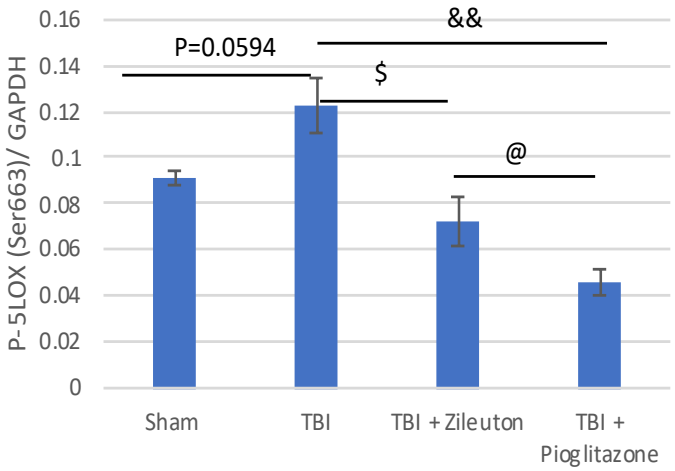

Figure 42C: A graph showing the protein expression of Phospho-5LOX (Serine 663) in isolated mixed glial cells, data were normalized to Total 5-LOX (not shown) and to GAPDH, data were assessed using a students T tests. Sham (n=4) vs TBI- untreated (n=4) P= 0.0594 TBI- untreated (n=4) vs TBI + Zileuton (n=4) P=0.0106 (Indicated by $). TBI- untreated (n=4 vs TBI + Pioglitazone (n=4) P= 0.0061 . TBI + Zileuton (n=4) vs TBI + Pioglitazone (n=4) P= 0.0356 (indicated by @). Error bars represent SEM.

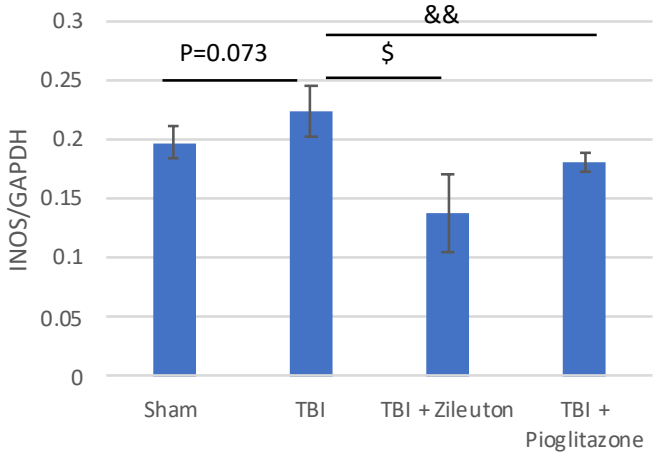

Figure 42D: A graph showing the protein expression of INOS in isolated mixed glial cells, data were normalized to GAPDH, data were assessed using a students T tests. Sham (n=4) vs TBI- untreated (n=4) P= 0.073, TBI- untreated (n=4 vs TBI + Zileuton (n=4) P= 0.0142 (Indicated by $). TBI- untreated (n=4 vs TBI + Pioglitazone (n=4) P= 0.0186 (Indicated by &&). TBI + Zileuton (n=4) vs TBI + Pioglitazone (n=4) P= 0.093 . Error bars represent SEM.

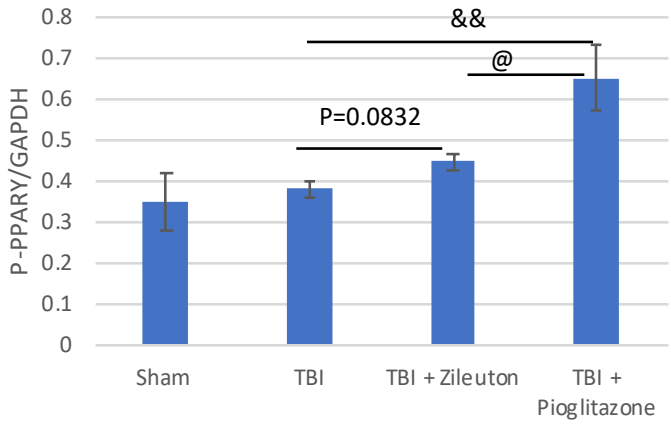

Figure 42E: A graph showing the protein expression of Phospho- PPARY (Serine 112) in isolated mixed glial cells, data were normalized to Total PPARY (not shown) and to GAPDH, data were assessed using a students T tests. Sham (n=4) vs TBI- untreated (n=4) P= 0.335 , TBI- untreated (n=4 vs TBI + Zileuton (n=4) P= 0.0832 (Indicated by $). TBI- untreated (n=4 vs TBI + Pioglitazone (n=4) P= 0.0080 (Indicated by &&). TBI + Zileuton (n=4) vs TBI + Pioglitazone (n=4) P= 0.0229 (Indicated by @). Error bars represent SEM.

Investigation of target engagement in glial cells - immediately after isolation – Figure 25A-B

Plan: Expose mice to r-sham/r-mTBI → Isolate mixed glia 24 hours post last-injury → Sample split into two (i) ½ received LPS @10ng/ml for 2 hours, (ii) half as a control cell culture media.

Analysis of glial response to LPS following isolation from injured or sham mice

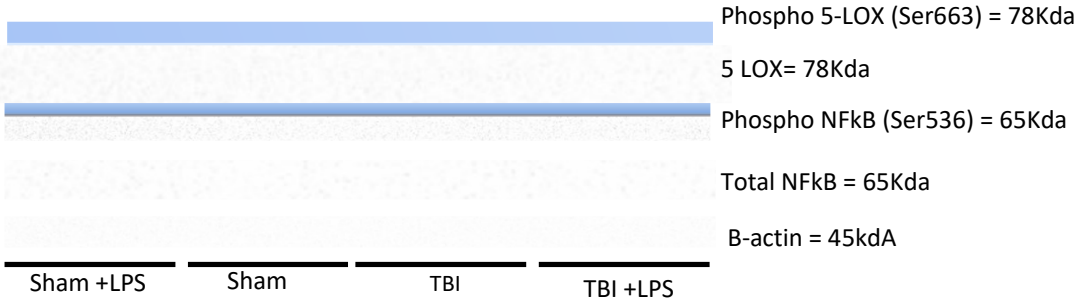

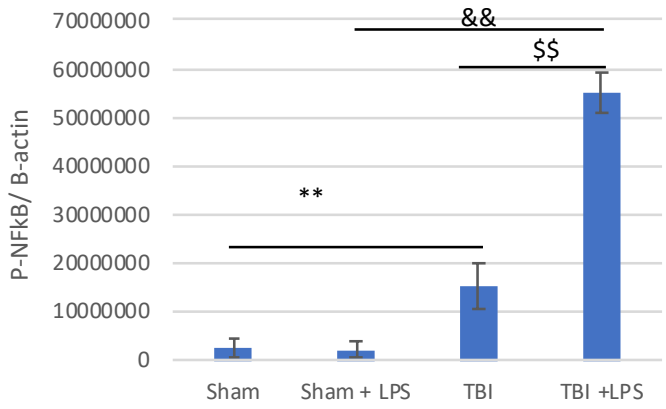

Figure 43A: *A graph showing the protein expression of Phospho-NFkB (Serine 536) in isolated mixed glial cells, data were normalized to Total NFkB and to B-actin, data were assessed using a students T tests. Sham (n=3) vs TBI-(n=3) P= 0.0085 (indicated by **), TBI(n=3) vs TBI+ LPS @10ng/ml (n=3) P= 0.00210 (Indicated by $$). TBI + LPS @10ng/ml (n=3) vs Sham+ LPS @10ng/ml (n=3) P= 0.00508(Indicated by &&). Error bars represent SEM.*

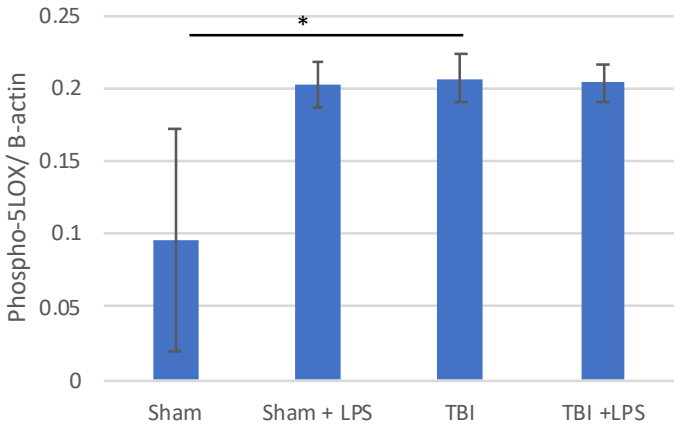

Figure 43B: *A graph showing the protein expression of Phospho-5LOX (Serine 663) in isolated mixed glial cells, data were normalized to Total 5-LOX and to B-actin, data were assessed using a students T tests. Sham (n=3) vs TBI-(n=3) P= 0.035 (indicated by *), TBI(n=3) vs TBI+ LPS @10ng/ml (n=3) P= 0.0877. TBI + LPS @10ng/ml (n=3) vs Sham+ LPS @10ng/ml (n=3) P= 0.136. Error bars represent SEM.*

Liraglutide (Figure 44A-I) and Bexarotene (45A-K) study – target engagement and impact on TBI mediated glial reactivity and white matter damage.

Liraglutide reduces TBI dependent increase in pNFKb/Total NFKb levels (Figure. 44A), and ameliorates IBA1+ microglial reactivity in the corpus callosum, hippocampus and cortex (Figure. 44D,F,H).

Indirect target engagement was observed downstream of GLP-1 receptor activity, by the upregulation or pCREB in TBI-treated mice vs TBI vehicle mice (Figure. 44C).

No effects were observed in the iNOS (Figure. 44E,G,I) or GFAP levels in all brain regions analyzed (Figure. 44E,44G,44I)

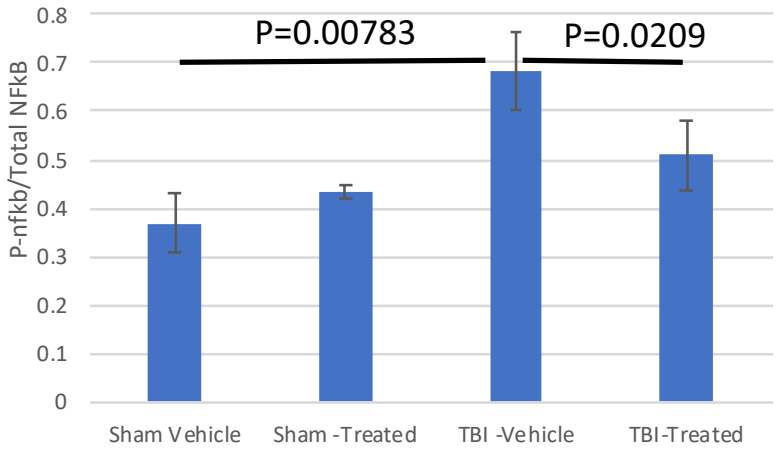

Figure 44A: graph showing the protein expression of Phospho- NFkB (Serine 536) in the cytoplasmic/ nuclear fraction of mouse cortex homogenate of sham or mTBI injured mice who either received vehicle or treatment with Liraglutide (n=4/group), data were normalized to Total NFkB and to B-actin. Sham untreated (n=4) vs TBI- untreated (n=4) P= 0.00783. TBI- untreated (n=4) vs TBI + Liragutide (n=4) P= 0.0209.. Error bars represent SD.

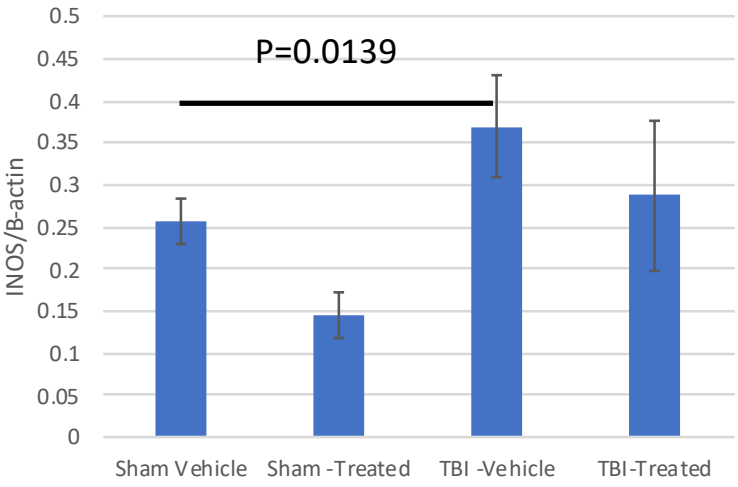

Figure 44B: graph showing the protein expression of Inducible Nitric oxide synthase (INOS) in the cytoplasmic /nuclear fraction of mouse cortex homogenate of sham or mTBI injured mice who either received vehicle or treatment with Bexarotene (n=4/group),, data were normalized to B-actin. Sham (n=4) vs TBI- untreated (n=4) P= 0.0783. TBI- untreated (n=4) vs TBI + Liragutide (n=4) P= 0.0209. Error bars represent SD.

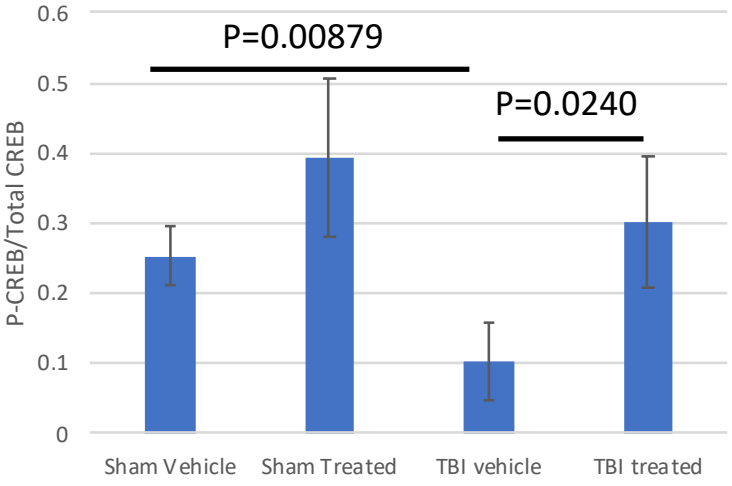

Figure 44C: graph showing the protein expression of Phospho- Cyclic response element binding protein (CREB) (Serine 133) in the cytoplasmic / nuclear fraction of mouse cortex homogenate, data were normalized to Total CREB and to B-actin. Sham (n=4) vs TBI- untreated (n=4) P= 0.00879. TBI- untreated (n=4) vs TBI + Liragutide (n=4) P= 0.0240. Error bars represent SD.

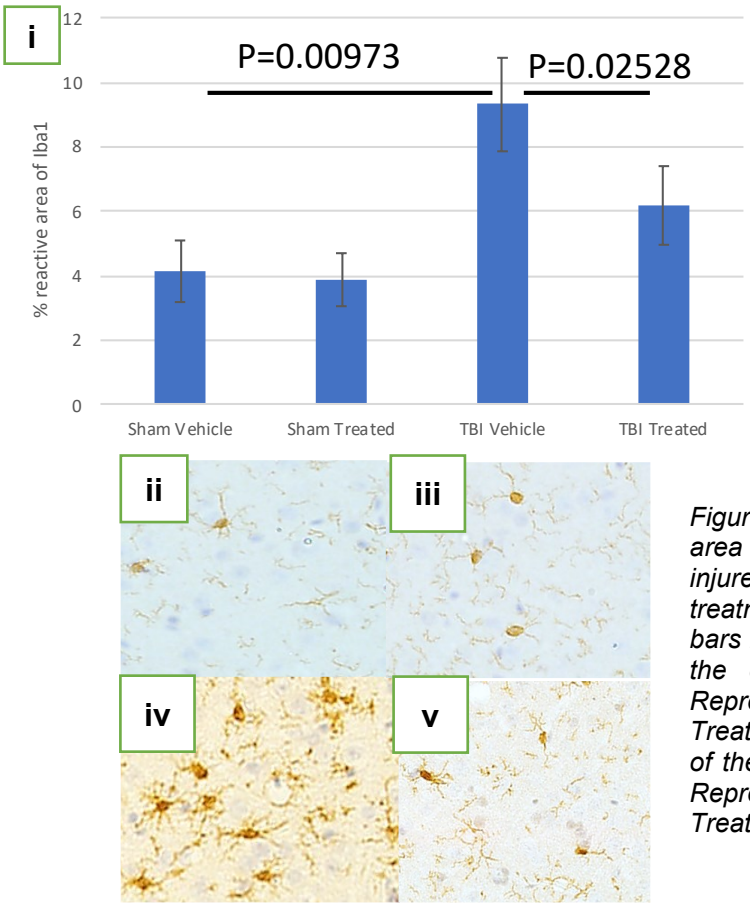

Figure 44D: (i) Graph showing the % reactive area of Iba1 in the cortex of sham or mTBI injured mice who either received vehicle or treatment with Liraglutide (n=6/group). Error bars represent SD. (ii) Representative image of the cortex of sham vehicle mice for Iba1. (iii) Representative image of the cortex of sham Treated mice for Iba1. (iv) Representative image of the cortex of TBI vehicle mice for Iba1. (v) Representative image of the cortex of TBI Treated mice for Iba1.

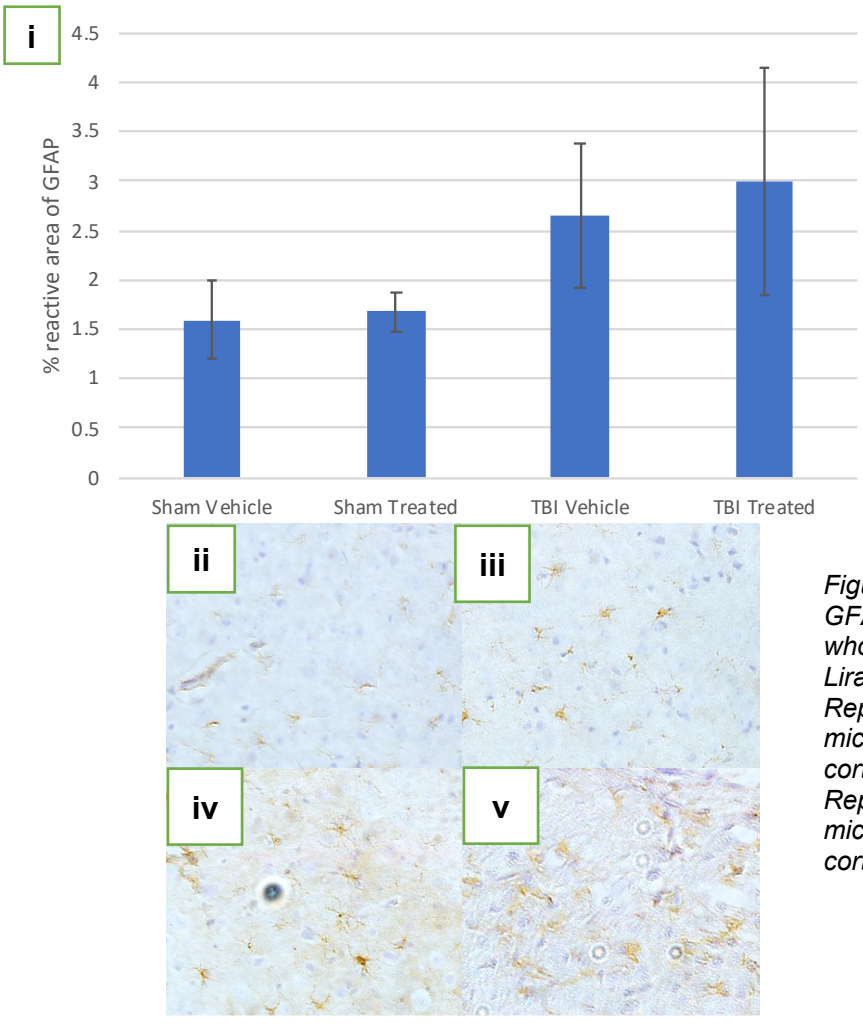

Figure 44E: (i) Graph showing the % reactive area of GFAP in the cortex of sham or mTBI injured mice who either received vehicle or treatment with Liraglutide (n=6/group). Error bars represent SD. (ii) Representative image of the cortex of sham vehicle mice for GFAP. (iii) Representative image of the cortex of sham Treated mice for GFAP. (iv) Representative image of the cortex of TBI vehicle mice for GFAP. (v) Representative image of the cortex of TBI Treated mice for GFAP.

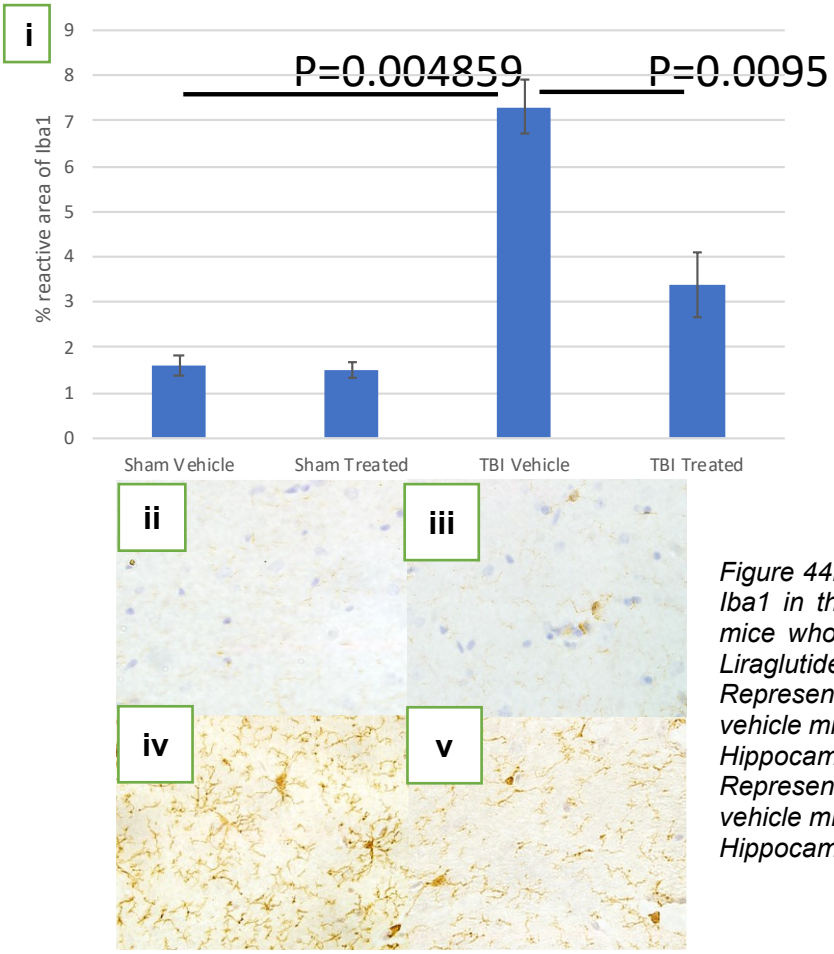

Figure 44F: (i) Graph showing the % reactive area of Iba1 in the Hippocampus of sham or mTBI injured mice who either received vehicle or treatment with Liraglutide (n=6/group). Error bars represent SD. (ii) Representative image of the Hippocampus of sham vehicle mice for Iba1. (iii) Representative image of the Hippocampus of sham Treated mice for Iba1. (iv) Representative image of the Hippocampus of TBI vehicle mice for Iba1. (v) Representative image of the Hippocampus of TBI Treated mice for Iba1.

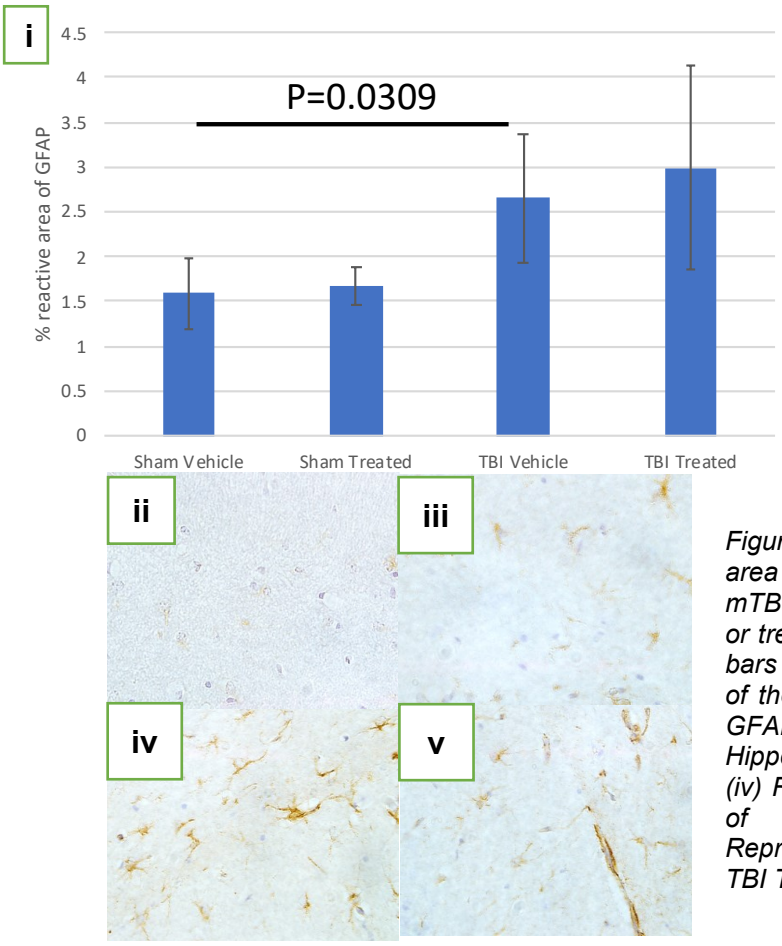

Figure 44G: (i) Graph showing the % reactive area of GFAP in the Hippocampus of sham or mTBI injured mice who either received vehicle or treatment with Liraglutide (n=6/group). Error bars represent SEM. (ii) Representative image of the Hippocampus of sham vehicle mice for GFAP. (iii) Representative image of the Hippocampus of sham Treated mice for GFAP. (iv) Representative image of the Hippocampus of TBI vehicle mice for GFAP. (v) Representative image of the Hippocampus of TBI Treated mice for GFAP.

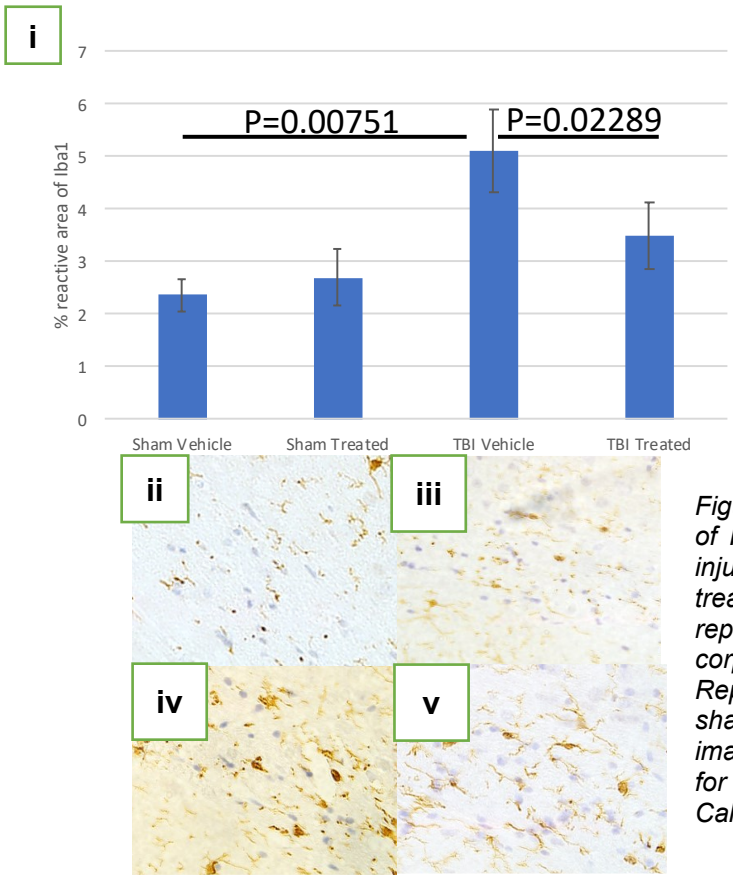

Figure 44H: (i) Graph showing the % reactive area of Iba1 in the Corpus Callosum of sham or mTBI injured mice who either received vehicle or treatment with Liraglutide (n=6/group). Error bars represent SD. (ii) Representative image of the corpus Callosum of sham vehicle mice for Iba1. (iii) Representative image of the corpus Callosum of sham Treated mice for Iba1. (iv) Representative image of the corpus Callosum of TBI vehicle mice for Iba1. (v) Representative image of the corpus Callosum of TBI Treated mice for Iba1.

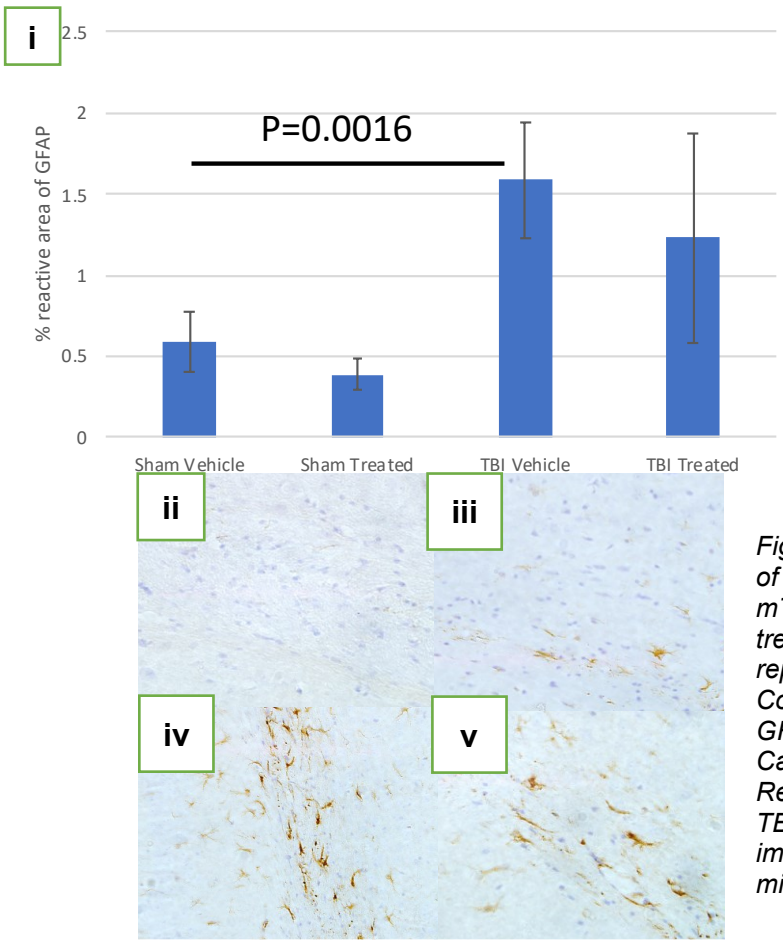

Figure 44I: (i) Graph showing the % reactive area of GFAP in the Corpus Callosum of sham or mTBI injured mice who either received vehicle or treatment with Liraglutide (n=6/group). Error bars represent SEM. (ii) Representative image of the Corpus Callosum of sham vehicle mice for GFAP. (iii) Representative image of the Corpus Callosum of sham Treated mice for GFAP. (iv) Representative image of the Corpus Callosum of TBI vehicle mice for GFAP. (v) Representative image of the Corpus Callosum of TBI Treated mice for GFAP.

Baxerotene upregulated RXRa receptor expression in the TBI-treated vs vehicle mice (Figure 45A).
No effect was observed for other related targets pPPARgamma and PGCA1 (Figure 45B,C).
No effect was observed for iNOS or pNFkB with treatment (Figure 45D-E).
Baxerotene did not ameliorate TBI dependent astroglia or microglia reactivity (Figure 45F-K).

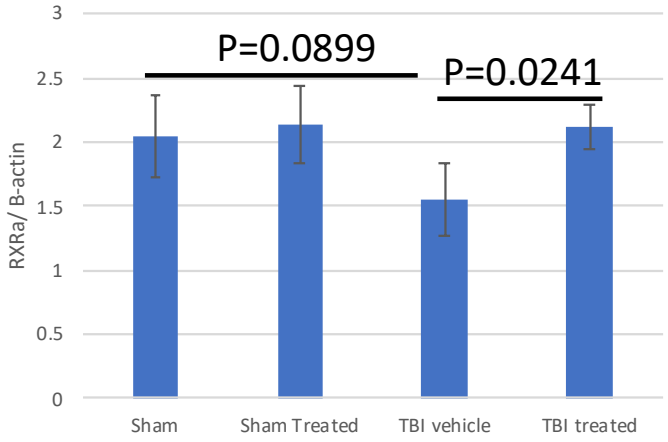

Figure 45A: graph showing the protein expression of Retinoid X Receptor in the cytoplasmic/ nuclear fraction of mouse cortex homogenate of sham or mTBI injured mice who either received vehicle or treatment with Bexarotene (n=4/group), data were normalized to Total NFkB and to B-actin. Sham untreated (n=4) vs TBI- untreated (n=4) P= 0.00783. TBI- untreated (n=4) vs TBI + Bexarotene(n=4) P= 0.0209. Error bars represent SD.

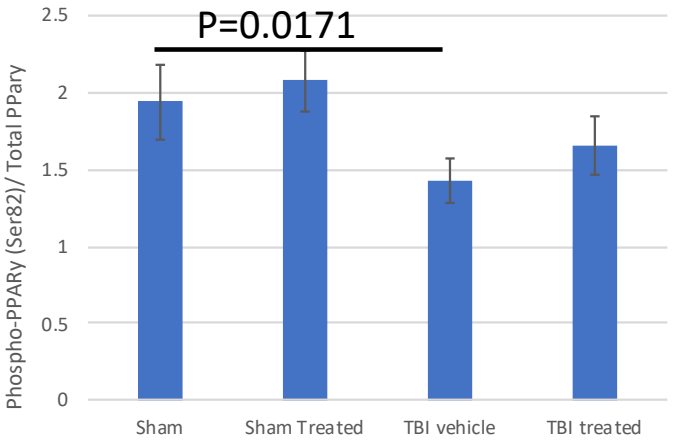

Figure 45B: graph showing the protein expression of phospho- Peroxisomal Proliferator Activated Recptor gamma (PPARy) in the cytoplasmic/ nuclear fraction of mouse cortex homogenate of sham or mTBI injured mice who either received vehicle or treatment with Bexarotene (n=4/group), data were normalized to Total NFkB and to B-actin. Sham untreated (n=4) vs TBI- untreated (n=4) P= 0.0171. Error bars represent SD.

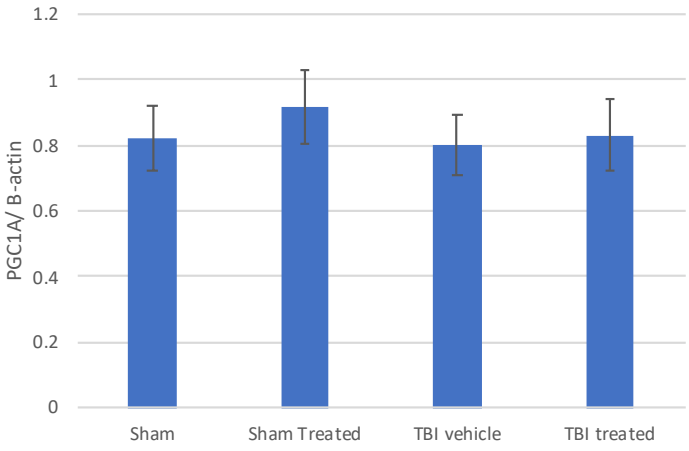

Figure 45C: graph showing the protein expression of Peroxisome co-activator group 1A (PGC1a) in the cytoplasmic/ nuclear fraction of mouse cortex homogenate of sham or mTBI injured mice who either received vehicle or treatment with Liraglutide (n=4/group), data were normalized to B-actin. Error bars represent SD.

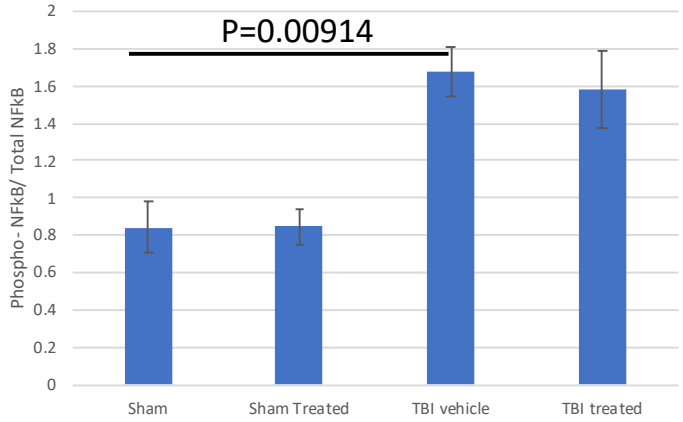

Figure 45D: graph showing the protein expression of Phospho- NFkB (Serine 536) in the cytoplasmic/ nuclear fraction of mouse cortex homogenate of sham or mTBI injured mice who either received vehicle or treatment with Liraglutide (n=4/group), data were normalized to Total NFkB and to B-actin. Sham untreated (n=4) vs TBI-untreated (n=4) P= 0.00914. Error bars represent SD.

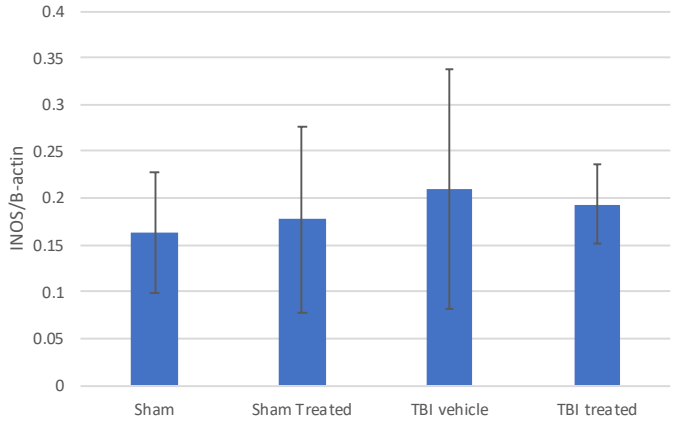

Figure 45E: graph showing the protein expression of Inducible Nitric oxide synthase (INOS) in the cytoplasmic /nuclear fraction of mouse cortex homogenate of sham or mTBI injured mice who either received vehicle or treatment with Bexarotene (n=4/group), data were normalized to B-actin. Sham (n=4) vs TBI- untreated (n=4) P= 0.0171. Error bars represent SD.

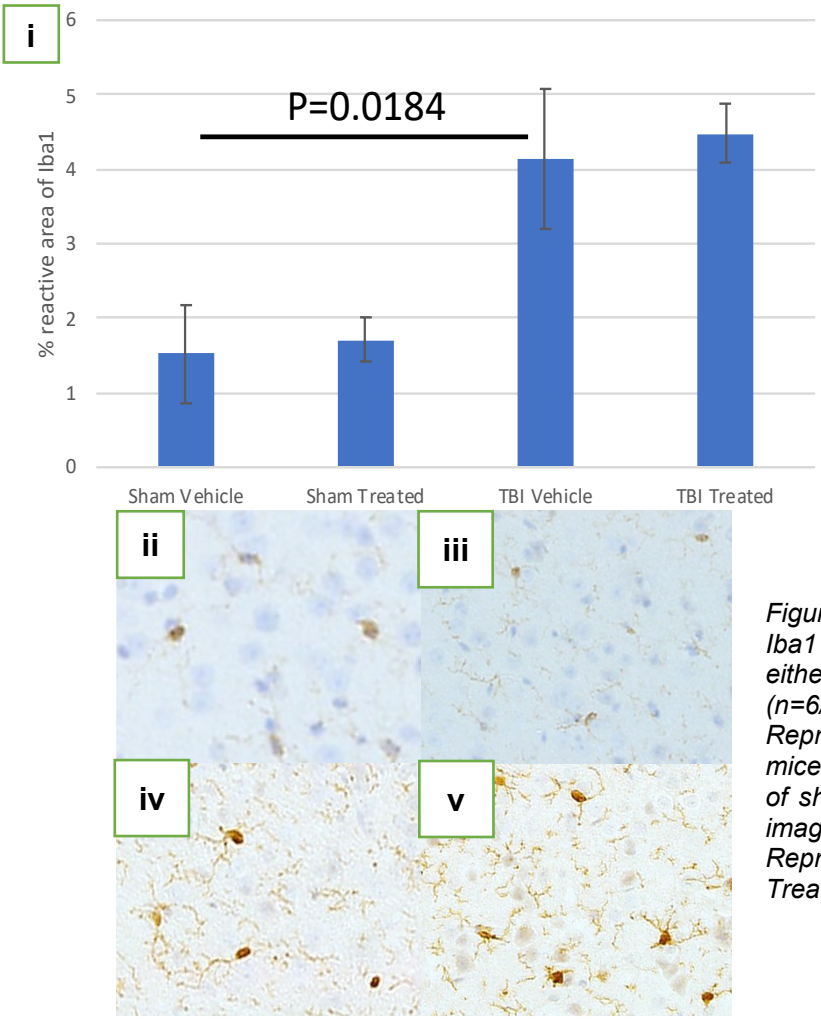

Figure 45G: (i) Graph showing the % reactive area of Iba1 in the cortex of sham or mTBI injured mice who either received vehicle or treatment with Bexarotene (n=6/group). Error bars represent SEM. (ii) Representative image of the cortex of sham vehicle mice for Iba1. (iii) Representative image of the cortex of sham Treated mice for Iba1. (iv) Representative image of the cortex of TBI vehicle mice for Iba1. (v) Representative image of the corpus Callosum of TBI Treated mice for Iba1.

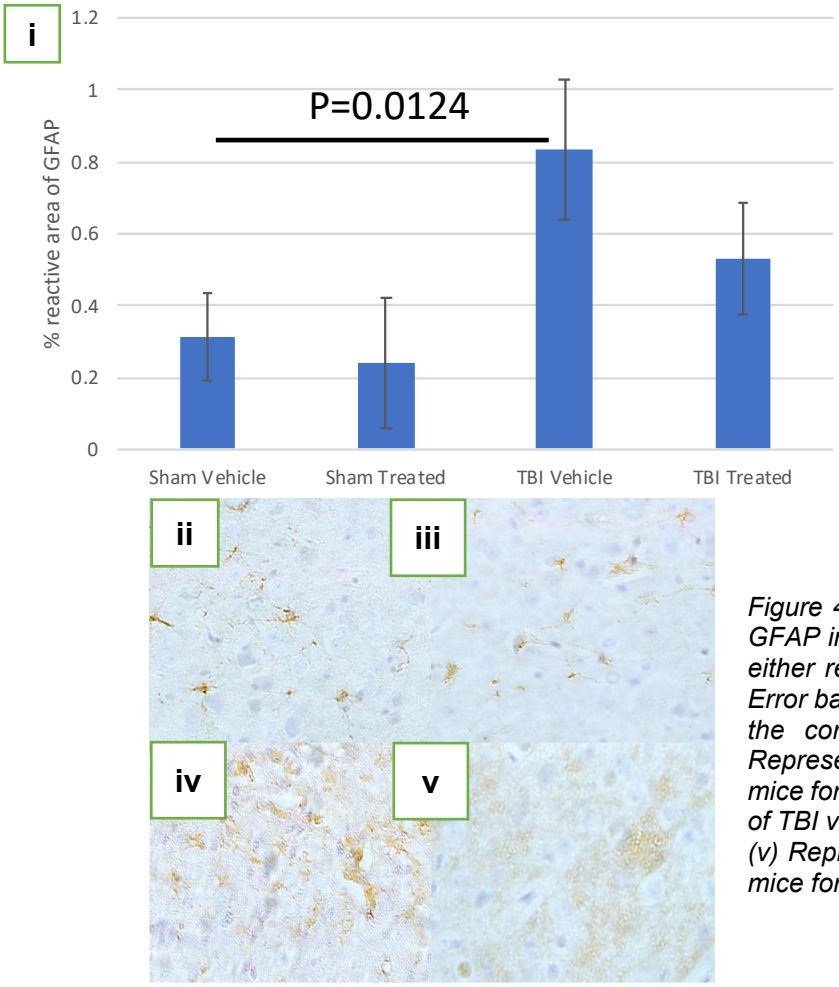

Figure 45H: (i) Graph showing the % reactive area of GFAP in the cortex of sham or mTBI injured mice who either received vehicle or treatment with Bexarotene. Error bars represent SEM. (ii) Representative image of the cortex of sham vehicle mice for GFAP. (iii) Representative image of the cortex of sham Treated mice for GFAP. (iv) Representative image of the cortex of TBI vehicle mice for GFAP.
(v) Representative image of the cortex of TBI Treated mice for GFAP.

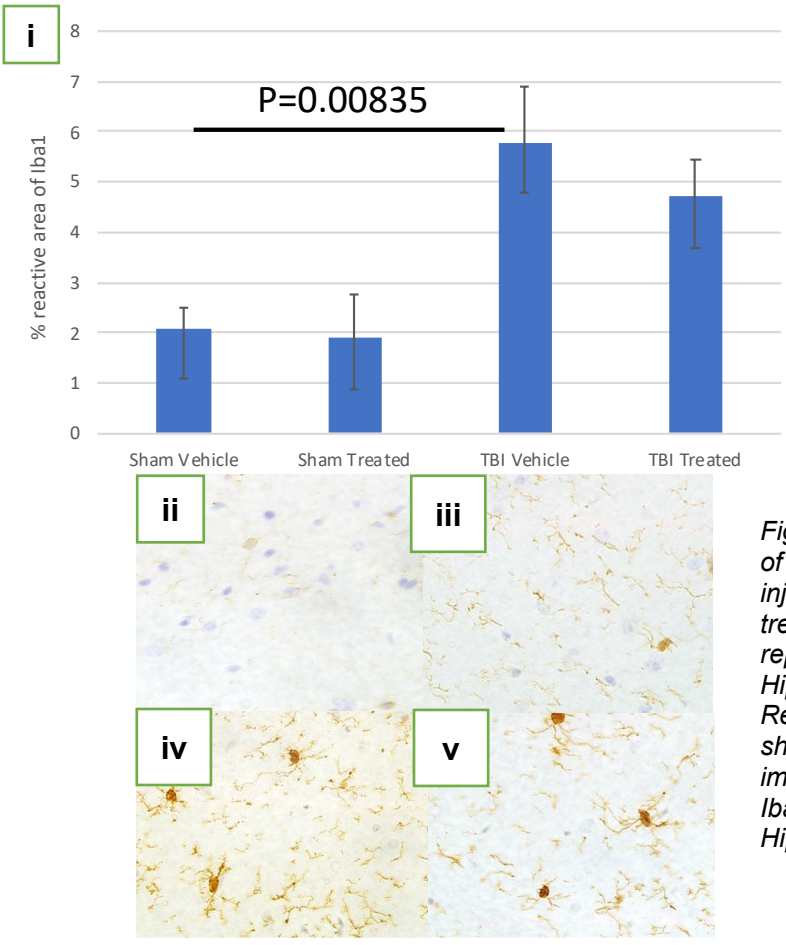

Figure 45H: (i) Graph showing the % reactive area of Iba1 in the Hippocampus of sham or mTBI injured mice who either received vehicle or treatment with Bexarotene (n=6/group). Error bars represent SD. (ii) Representative image of the Hippocampus of sham vehicle mice for Iba1. (iii) Representative image of the Hippocampus of sham Treated mice for Iba1. (iv) Representative image of the Hippocampus of TBI vehicle mice for Iba1. (v) Representative image of the Hippocampus of TBI Treated mice for Iba1.

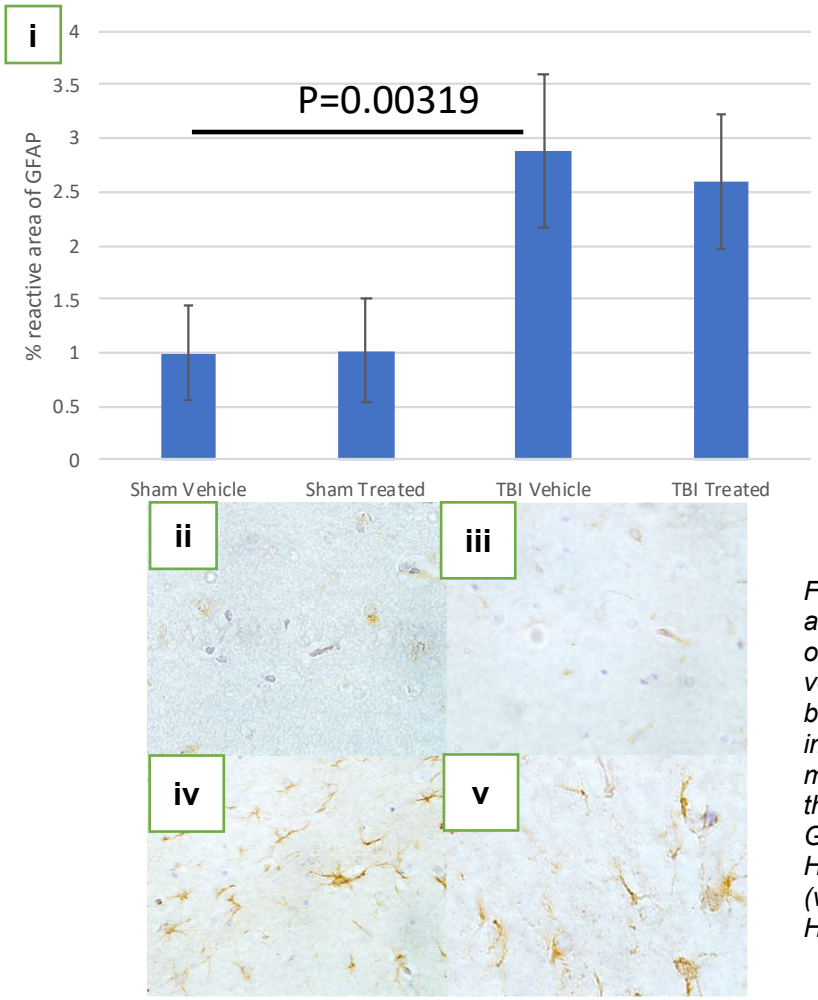

Figure 45I: (i) Graph showing the % reactive area of GFAP in the Hippocampus of sham or mTBI injured mice who either received vehicle or treatment with Bexarotene. Error bars represent SEM. (ii) Representative image of the Hippocampus of sham vehicle mice for GFAP. (iii) Representative image of the Hippocampus of sham Treated mice for GFAP. (iv) Representative image of the Hippocampus of TBI vehicle mice for GFAP. (v) Representative image of the Hippocampus of TBI Treated mice for GFAP.

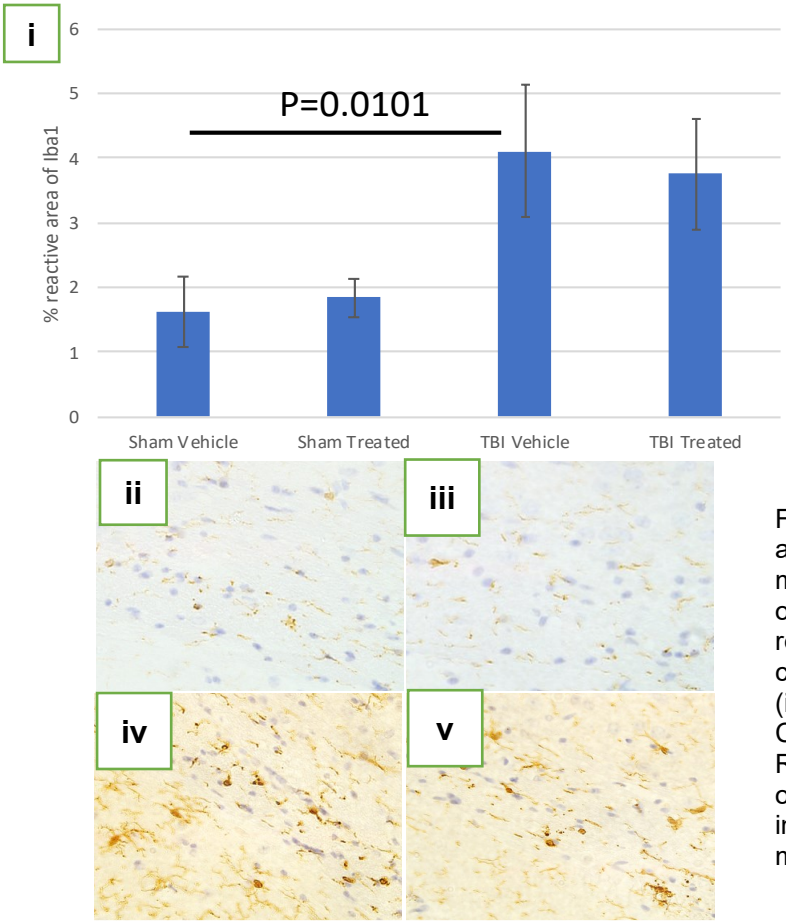

Figure 45J: (i) Graph showing the % reactive area of Iba1 in the corpus callosum of sham or mTBI injured mice who either received vehicle or treatment with Bexarotene. Error bars represent SEM. (ii) Representative image of the corpus Callosum of sham vehicle mice for Iba1. (iii) Representative image of the corpus Callosum of sham Treated mice for Iba1. (iv) Representative image of the corpus Callosum of TBI vehicle mice for Iba1. (v) Representative image of the corpus Callosum of TBI Treated mice for Iba1.

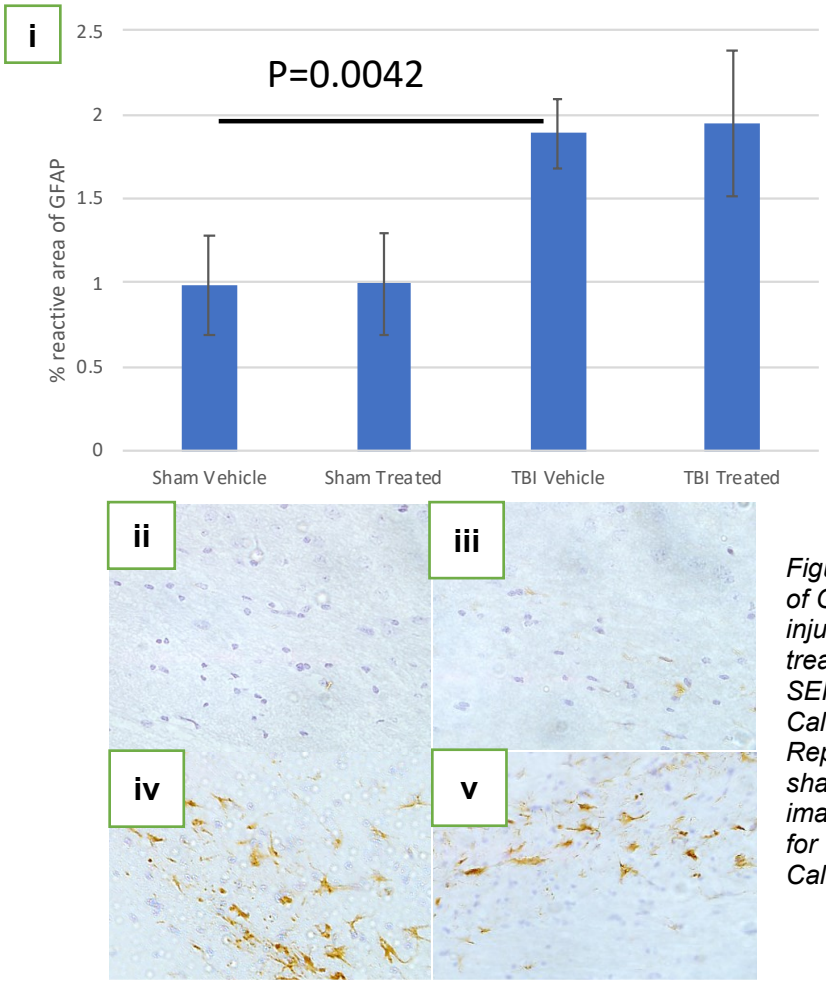

Figure 45K: (i) Graph showing the % reactive area of GFAP in the Corpus Callosum of sham or mTBI injured mice who either received vehicle or treatment with Bexarotene. Error bars represent SEM. (ii) Representative image of the Corpus Callosum of sham vehicle mice for GFAP. (iii) Representative image of the Corpus Callosum of sham Treated mice for GFAP. (iv) Representative image of the Corpus Callosum of TBI vehicle mice for GFAP. (v) Representative image of the Corpus Callosum of TBI Treated mice for GFAP.

Score sheet evaluation

Compound name	Evidence of target engagement on primary target	Evidence of pathological benefit	In both Iba1 and GFAP?	Evidence of anti-inflammatory potential (P-NFKB)	Ease of administration	Potential harmful side effects?	Total points
Zileuton	5-Lipoxygenase inhibitor- YES +2	Yes	yes +2	yes +2	In water +2	known issue of raised liver enzymes +0	8
Montelukast	Cys LT1 receptor antagonist- No +0	Yes	no- GFAP only +1	yes +2	In water +2	Known issue with Nausea +0	5
Fingolimod	S1P1-receptor agonist- No +0	no	N/A +0	no +0	In water +2	Increased risk of infections +0	2
7'8-DHF	TrkB receptor agonist - Yes +2	yes	no- GFAP only +1	no +0	In water +2	No serious risks reported +1	6
Pioglitazone	PPARγ agonist- Yes +2	Yes	yes +2	yes +2	In chow +2	Increased risk of hepatocellular carcinoma +0	8
Insulin	AKT/PI3K pathway activation- NO +0	no	N/A +0	no +0	Intranasal +1	No serious risks reported +1	1
Bexarotene	RxR agonist –Yes +2	no	N/A +0	no	In water +2	No serious risks reported +1	5
Liraglutide	GLP1r agonist – Phospho CREB as a surrogate target – Yes +2	Yes	no- Iba1 only +1	yes +2	Intraperitoneal +0	Increased risk of malignant thyroid cancers * (in animal models)+0	5
PTEN KO							

Top targets: 5-LOX, PPARgamma

CONCLUSION

- Completed major aspects of our first aim.
- We validated our main targets in human autopsy TBI and AD tissue to demonstrate human relevance.
- Development mass spectrometry protocol for measuring bioactive lipids in the brain tissue and isolated single cells of TBI vs sham mice to validate changes in downstream bioactive lipids related to the eicosanoid pathways.

- Developed a single cell isolation method for extracting glial cells for interrogation of cell specific effects in our model which we plan to use for single cell proteomic and lipidomic analyses of our compounds in microglia and astrocytes for our long-term treatment study.
- We have developed as part of this project an additional in vitro screening platform for our compounds in astrocyte, microglia and neuronal cell lines. We will utilize this platform as an additional validation step in the selection of our top performing compounds prior to initiating our long term treatment studies in Aim 2
- Completed interrogation of target engagement and therapeutic efficacy of Monteleukast (leukotriene receptor antagonist), Zileuton (5-lipo-oxygenase inhibitor), flavonoid 7,8-dihydroxyflavone (BDNF receptor-TrkB agonist), and Fingolimod (sphingosine-1-phosphate receptor modulator), Oleoylethanolamide (PPAR alpha agonist), Pioglitazone (PPAR gamma agonist), intranasal insulin, Baxerotene (RXR agonist) and Liraglutide (IGF1/GLP-1).
- We have ranked the list of different compounds and have selecting 5-lox, PPARg as the best performing targets thus far. We are still attempting to select one final target to move forward for Aim 2 studies.
- We are currently breeding and ageing mice, and planning administration of injuries for the start of studies in Major Task 2, where we will administer the top 3 performing compounds in a longer treatment regimen.

What opportunities for training and professional development has the project provided?

Nothing to Report

How were the results disseminated to communities of interest? Nothing to report

What do you plan to do during the next reporting period to accomplish the goals?

We are breeding and ageing mice, and planning administration of injuries for the start of studies in Major Task 2, where we will administer the top 3 performing compounds in a long-term treatment regimen that will be initiated 3 months post-injury and last for 6 months until euthanasia. In this study we will conduct behavioral, neuropathological, and biochemical analyses to asses efficacy of our compounds.

We plan to accomplish subtasks 1, and begin studies in subtask 2 during the next quarter.

Subtask 1: Administration of r-mTBI or r-sham injury to 180 male hTau mice at 2-3 months of age (60 mice per group)
Animals will receive closed head injuries over a 1 month period.

For each of 3 potential therapeutics there will be 6 groups– [r-mTBI treated low dose; r-mTBI treated high dose; r-mTBI vehicle; r-sham treated low dose; r-sham treated high dose; r-sham vehicle] each with 10 hTau mice

Subtask 2: Administration of therapeutic compounds to hTau mice for 6 months beginning at 3 months post TBI/sham.
Subtask 2a: Administration of Top performing therapeutic compound I
Subtask 2b: Administration of Top performing therapeutic compound II
Subtask 2c: Administration of Top performing therapeutic compound III

4. IMPACT:

What was the impact on the development of the principal discipline(s) of the project?

Nothing to Report.

What was the impact on other disciplines? Nothing to Report

What was the impact on technology transfer? Nothing to Report

What was the impact on society beyond science and technology? Nothing to Report

5. CHANGES/PROBLEMS:

Changes in approach and reasons for change

We are considering the use of conditional mice for one of our targets in Major Task 2, if we are unable to identify a suitable route of administration for our chosen compound during the proposed 6 months duration of treatment. Conditional models which can be regulated by doxycycline treatment may provide a means for avoiding this situation. Should this be the case, we will make minor adjustments to the animal protocol and begin breeding animals immediately. No changes will be made to the TBI paradigm or treatment regimen.

Actual or anticipated problems or delays and actions or plans to resolve them

Our ACURO protocol was accepted in late March 2018, and we also sent in an additional amendment to include the use of C57BL6 mice for our acute treatment studies and to replace our TBI paradigm to a more chronic r-mTBI model. We anticipate that this will set us back by a few months from our initial timeline, and we anticipate generating all the data in Major Tasks Two, 4-6 months later than our initial schedule in the statement of work. We plan to request for a 6 month extension for the project, with not budgetary changes. Apart from this set back we do not anticipate any new problems going forward.

Changes that had a significant impact on expenditures Nothing to Report

Significant changes in use or care of human subjects, vertebrate animals, biohazards, and/or select agents Nothing to report

Significant changes in use or care of human subjects: Nothing to Report

Significant changes in use or care of vertebrate animals: Nothing to Report

Significant changes in use of biohazards and/or select agents: Nothing to Report

6. PRODUCTS

Publications, conference papers, and presentations

Poster presentation: Pearson A, Burca I, Algamal I, Abdullah L, Evans J, Ojo J, Crawford F. Pharmacological blockade of leukotriene synthesis ameliorates neuroinflammation and reactive gliosis following repetitive mTBI. *National Neurotrauma Society conference 2019 (Pittsburgh).*

Journal publications. Nothing to Report (In preparation)
Books or other non-periodical, one-time publications. Nothing to Report
Other publications, conference papers, and presentations. *Nothing to Report*

Website(s) or other Internet site(s) *Nothing to Report*
Technologies or techniques *Nothing to Report*
Inventions, patent applications, and/or licenses *Nothing to Report*
Other Products *Nothing to Report*

7. PARTICIPANTS & OTHER COLLABORATING ORGANIZATIONS

What individuals have worked on the project?

Personnel	Researcher Identifier	Nearest Person Month Worked	Contribution to Project	Funding Support
Dr. Fiona Crawford	N/A	1	Principal Investigator	N/A
Dr. Joseph Ojo	N/A	2	Co-Principal Investigator	N/A
Dr. Benoit Mouzon	N/A	0.5	Co-Investigator – TBI animal models	N/A
Dr. Daniel Paris	N/A	0.5	Co-Investigator – Drug Discovery	N/A
Dr. Laila Abdullah	N/A	0.5	Co-Investigator - Lipidomics	N/A
James Evans	N/A	0.5	Consultant – lipid biology	N/A
Dr. Michael Mullan	N/A	0.5	Consultant	N/A
Andrew Pearson MS	N/A	6	Consultant	N/A

Has there been a change in the active other support of the PD/PI(s) or senior/key personnel since the last reporting period? None

What other organizations were involved as partners? Nothing to Report

8. SPECIAL REPORTING REQUIREMENTS

COLLABORATIVE AWARDS: *N/A*

QUAD CHARTS: *(Attached)*

9. APPENDICES – See attached Quad Chart

Novel Therapeutic Target Identification through analysis of Convergent AD and TBI Pathogenic Mechanisms

Log Number AZ160110

W81XWH-17-1-0638

PI: Drs Fiona Crawford / Joseph Ojo **Org:** The Roskamp Institute, Inc., Sarasota, FL **Award Amount:** $800,000

Study Aim(s)

Aim 1: Validation of potential targets for therapeutic intervention in the pathogenic TBI-AD interrelationship - eicosanoid signaling, PI3-kinase/Akt /PTEN/mTOR/insulin signaling and RXR/PPAR pathway.

Aim 2: Chronic evaluation of the efficacy of three potential therapeutics against the pathogenic TBI-AD interrelationship

Approach

i) Evaluate target engagement and efficacy in recovering normal molecular profiles in TBI mice using compounds that modulate the TBI and AD coincident molecular changes in a short-term (2wks) treatment Paradigm

ii) In vivo validation of therapeutic targets in mice with TBI using chronic intervention (6-month treatment regimen) with the top three performing compounds for three different targets from Aim 1 to evaluate the long-term neurobehavioral, neuropathological and biochemical outcomes

iii) Selection of downstream convergent tractable targets between the three different compounds for further exploration.

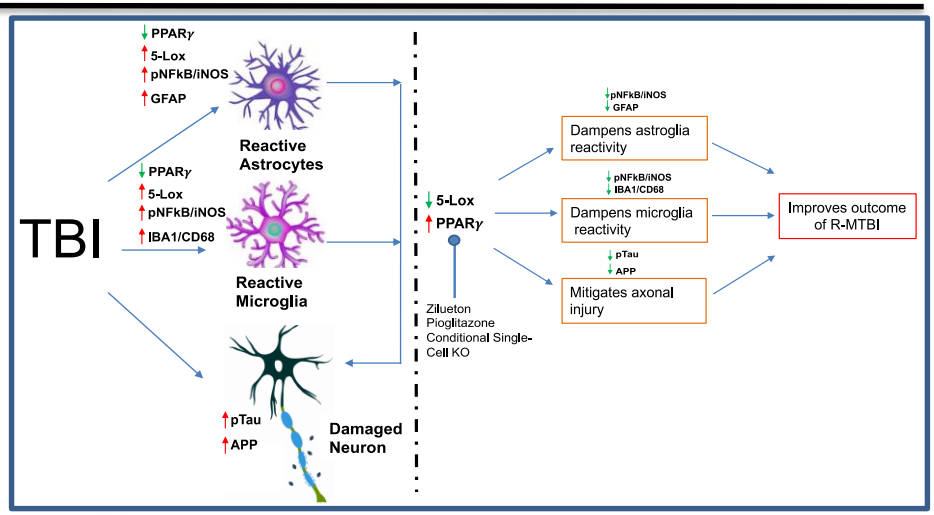

Accomplishment

Completed interrogation of target engagement/efficacy of 8 drugs in TBI, and selected 5-LOX and PPARγ as the best targets for further exploration. We also developed a single cell Omics platform to assess effect of compounds on microglia and astrocytes.

Timeline and Cost

Activities CY	18	19	20
MAJOR TASK ONE OR AIM 1			
MAJOR TASK TWO OR AIM 2			
Estimated Direct Budget (500K)	**$180K**	**$150K**	**$170K**

Last updated: (September 2017)

Goals/Milestones

CY17 Goal

☑ Obtain regulatory approval to begin animal studies

☑ Validate identified targets in mouse and human TBI/AD brains

CY18 Goals

☑ Initiate short treatment study to evaluate target engagement and efficacy

CY19 Goals

☑ Evaluate and select Top performing therapeutics for use in Aim 2

☑ Initiate chronic treatment study with the Top 3 performing compounds

CY20 Goal

❑ Complete chronic treatment study and evaluate the neurobehavioral, neuropathological and biochemical outcomes

Comments/Challenges/Issues/Concerns

- 4-6 Months behind schedule due to lag in time for ACURO review
- Generating conditional mice to evaluate targets for compounds with poor route of administration for the chronic study

Budget Expenditure to Date

Projected Expenditure: $528,739.78 Actual Expenditure: $375,321.42